



The maize *premature senescence2* encodes for *PHYTOCHROME-DEPENDENT LATE-FLOWERING* and its expression modulation improves agronomic traits under abiotic stresses

Rajeev Gupta | Shuping Jiao | Suling Zhao | Robert B. Meeley |
Robert W. Williams | Graziana Taramino | Dongsheng Feng | Guofu Li |
Juan Liu | Stephen M. Allen | Kevin D. Simcox | Dilbag S. Multani

Corteva Agriscience, Johnston, IA, USA

Correspondence

Dilbag S. Multani, Napigen Inc., 200 Powder Mill Road, Delaware Innovation Space, E-400, Wilmington, DE 19803, USA.
Email: dilbagmultani8@gmail.com

Present address

Rajeev Gupta, International Crops Research Institute for the Semi-Arid Tropics (ICRISAT), Patancheru, TS, India
Suling Zhao and Graziana Taramino, Bayer Crop Science, Chesterfield, MO, USA
Robert B. Meeley, Des Moines, IA, USA
Robert W. Williams, Calyxt, Roseville, MN, USA
Dongsheng Feng, Kekaha, HI, USA
Guofu Li, Bellagen, Qilu Innovalley Incubator, High-Tech Industry Development Zone, Jinan, Shandong, China
Juan Liu, Gene Therapy Program, University of Pennsylvania, Philadelphia, PA, USA
Stephen M. Allen, Wilmington, DE, USA
Kevin D. Simcox, West Des Moines, IA, USA
Dilbag S. Multani, Napigen Inc., Delaware Innovation Space, Wilmington, DE, USA

Funding information

Corteva Agriscience

Abstract

Among the various abiotic stresses, water and nitrogen are major stress factors that limit crop productivity worldwide. Since leaf nutrients remobilization during leaf senescence might impact response to abiotic stress in crops, we undertook a forward screen of the *Mutator*-active approach to identify *premature senescence* loci in maize. A mutant line isolated from a cross between a Pioneer Brand elite line and a public *Mutator*-active material, designated *premature senescence2* (*pre2*), expressed leaf senescence during flower initiation. The *Pre2* gene encodes PHYTOCHROME-DEPENDENT LATE-FLOWERING (PHL) protein, a nuclear receptor coactivator. The *pre2-1* mutant allele was not a null mutation but produced a functional wild-type transcript along with multiple mRNA species of varying lengths resulting from the alternate splicing of the *Pre2* gene. The PHL accelerates flowering by suppressing the inhibitory effect of *phyB* on flowering in Arabidopsis (Endo et al., 2013). The ZmPRE2 polypeptide is highly conserved in plant species and has two identifiable motifs namely SPT20 and MED15. The Spt20 domain, which is a part of the SAGA (Spt-Ada-Gcn5 acetyltransferase) complex, is involved in histone deacetylation and MED15 proteins have nuclear functions in mediating DNA Pol II transcription. The differential spliced mature transcripts in both the *pre2* alleles, as a result of transposon interference, were producing truncated proteins that lacked polyglutamine (Q) tract near the C-terminus and might be causative of the premature senescence phenotype in maize. Endogenous gene suppression of *ZmPre2* by RNAi improves maize agronomic performance under both water stress and suboptimal nitrogen conditions. The homozygous T-DNA knockout of the *pre2* homolog in Arabidopsis (At1G72390; the same insertional allele used by Endo et al., 2013) results in higher biomass, delayed maturity, enhanced tolerance to drought, and improved nitrogen utilization efficiency. The Arabidopsis mutant also showed hypersensitive response to 1 μ M ABA

Rajeev Gupta and Dilbag S. Multani are Senior authors.

This is an open access article under the terms of the Creative Commons Attribution-NonCommercial-NoDerivs License, which permits use and distribution in any medium, provided the original work is properly cited, the use is non-commercial and no modifications or adaptations are made.

© 2020 Corteva Inc Johnston Global Business Center. *Plant Direct* published by American Society of Plant Biologists and the Society for Experimental Biology and John Wiley & Sons Ltd.

(abscisic acid) concentration. These results indicate that the PHL protein plays a direct or indirect role in ABA-dependent drought and N signaling pathways.

KEYWORDS

drought tolerance, nitrogen use efficiency, senescence, transgene

1 | INTRODUCTION

Natural senescence is a programmed gradual deterioration of cellular function throughout the plant's lifespan (Himelblau & Amasino, 2001; Lim et al., 2007; Woo et al., 2019). This process is important for recycling resources, particularly nitrogen and carbon, to newly developing organs or storage sinks, thereby contributing to the fitness of a plant. Premature senescence, moreover, is a highly regulated process that is triggered in response to various environmental stimuli including biotic and abiotic stresses, such as temperature, nutrition, and light. Since leaf senescence results in loss of photosynthetic activity, delaying senescence can potentially enhance carbon assimilation and result in increased grain and biomass yield (Zhang et al., 2019). In addition, higher accumulation of photosynthates in vegetative plant parts may also result in value-added feedstocks and higher biofuel production. Elucidation of the molecular mechanisms underlying senescence has been facilitated by advances in forward and reverse genetics, resulting in the cloning and characterization of senescence-related genes from the number of species (Buchanan-Wollaston et al., 2003; for review, see Lim et al., 2007). Similarly, the latest advances in genome sequencing, molecular markers, genome-wide association studies (GWAS), and gene expression profiling have identified senescence-associated genes (SAGs), and differentially expressed genes (DEGs), that are up- and down-regulated during natural and induced senescence (Breeze et al., 2011; Buchanan-Wollaston et al., 2005; Chai et al., 2019; van der Graaff et al., 2006; Guo et al., 2004; Liu et al., 2011; Sekhon et al., 2019).

Of the many factors affecting crop yield, improvement of agronomic traits in crop plants growing under both optimal and sub-optimal environmental conditions are particularly beneficial to farmers. Abiotic stress is the primary cause of crop loss worldwide, causing average yield losses of more than 50% for major crops. Among the various abiotic stresses, drought is a major factor that limits crop productivity worldwide (Bot et al., 2000). Exposure of plants to a water-limiting environment during various developmental stages activates various physiological and developmental changes. Molecular mechanisms of abiotic stress responses and the genetic regulatory networks of drought stress tolerance have been documented (Sade et al., 2018). Natural responses to abiotic stress vary among plant species and among varieties and cultivars within a plant species. Transgenic approaches, including gene overexpression or downregulation, are being evaluated for engineering drought tolerance in crop plants (Brugière et al., 2017; Deikman et al., 2012; Shi et al., 2015).

Similarly, Nitrogen (N) is a major limiting factor in plant productivity. Increased N fertilizer application underlies the substantial increase in global agricultural food production over the last half

century (Omara et al., 2019). Improving N use efficiency (NUE) of crop plants through efficient removal from the soil and better utilization for faster growth can help to reduce the amount of N application needed for maximal productivity as well as increase the profitability of the farmer and mitigating adverse environmental effects. Attempts to develop crop plants with enhanced NUE using more classical genetic approaches based on utilizing existing allelic variation for NUE traits are described (Han et al., 2015). World cereal NUE has also been slightly improved in the last two decades from 33% in 1999 to 35% in 2015 as compared to a maximum of 41% in the United States (Omara et al., 2019). NUE also affects yield, especially where the application of nitrogen fertilizer is limited. Thus, genes involved in NUE may affect crop yield and have utility for improving the use of nitrogen in crop plants, especially maize (*Zea mays* L.). The crucial components involved in N utilization and the candidate genes with the potential for NUE improvement in dicot *Arabidopsis* (*Arabidopsis thaliana*) and monocot rice (*Oryza sativa*) are summarized by Li et al. (2017). Increased NUE can result from enhanced the uptake and assimilation of nitrogen fertilizer, the subsequent remobilization and reutilization of accumulated nitrogen reserves, and increasing tolerance of plants to stress situations such as low Nitrogen environments (Low N). Improving NUE in maize would increase harvestable yield per unit of input nitrogen fertilizer, both in developing nations where access to nitrogen fertilizer is limited and in developed nations where the level of nitrogen use remains high (Han et al., 2015).

Since leaf nutrient remobilization might impact response to abiotic stress in crops, we undertook a forward screen of *Mutator*-active (*Mu*) transposon populations in maize to identify *premature senescence* loci. A novel premature senescence mutation was identified which expressed leaf senescence during flower initiation. This mutation was designated as *premature senescence2* (*pre2*). The *pre2* candidate gene encodes a PHYTOCHROME-DEPENDENT LATE-FLOWERING (PHL) protein, a nuclear receptor coactivator that had already been characterized in *Arabidopsis* through physical interactions with phytochrome B and CONSTANS (Endo et al., 2013). The PRE2 polypeptide has an Spt20 domain, found in the Spt20 family of proteins in both humans and yeast, which is a part of the SAGA (Spt-Ada-Gcn5 acetyltransferase) complex that may be involved in histone deacetylation. Here, we report that suppression of the endogenous *Pre2* gene by RNAi improves agronomic performance under water stress and in suboptimal nitrogen conditions in maize. The homozygous knockout of the *pre2* homolog in *Arabidopsis* results in higher biomass, late-flowering, enhanced tolerance to drought, and improved nitrogen utilization. In addition, the *Atpre2-KO* (*phl*) also showed hypersensitive response to 1 μ M abscisic acid (ABA).

Taking together these results indicate that the PHL plays additional direct or indirect roles in ABA-dependent drought and N signaling pathways.

2 | RESULTS

2.1 | Isolation and characterization of a *pre2* mutation in maize

A *premature senescence* mutant isolated from an F2 population of public *Mu*-active lines crossed with a Pioneer Brand elite

non-stiff stalk (NSS) inbred line expressed a leaf senescent phenotype 2–3 weeks prior to anthesis. Like natural senescence, the mutant phenotype starts from the lowermost leaves and then spreads to the top of the plant in a progressive fashion (Figure 1a). A total number of 176 plants, comprising of 41 mutants and 135 WT from the BC3F2 segregating population were used to map the mutation using 4K Illumina Array markers. The segregation of the mutant fits well in 1:3 ratio, indicating that the *premature senescence* mutant is controlled by a single recessive locus ($\chi^2 = 0.273$), and the marker data analysis placed this mutation to a 9.02cM interval between 187.63 and 196.65cM on chromosome 4 on the Corteva Agriscience genetic map. Reciprocal crosses of the new premature senescence

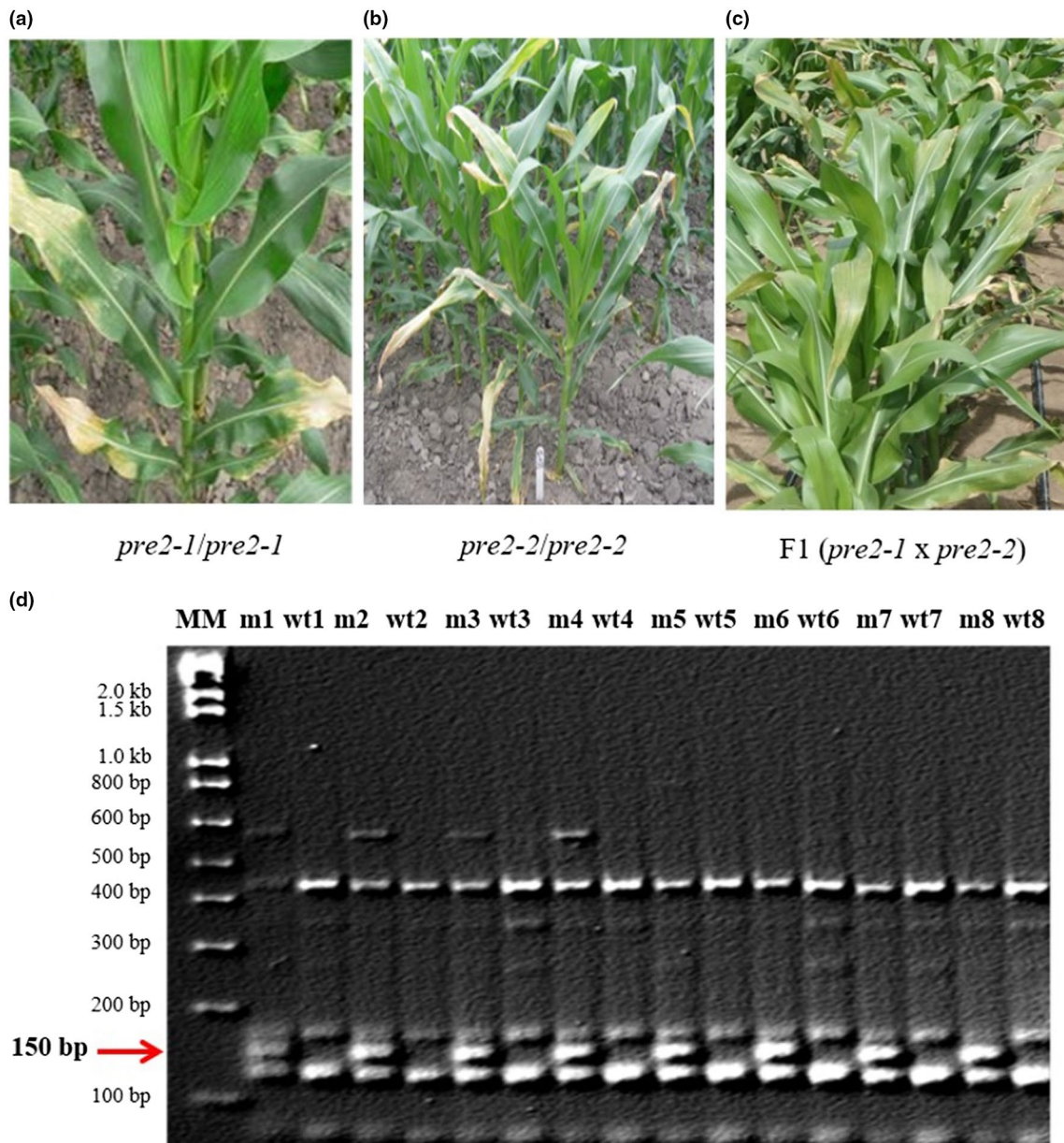


FIGURE 1 Phenotype and co-segregation analysis of the *pre2* mutation. (a) Homozygous *pre2-1* mutant; (b) homozygous *pre2-2* mutant; and (c) the *pre2-1/pre2-2* allelic cross. (d) Co-segregation analysis of the *pre2-1* mutant using a modified PCR-based SAIFA analysis in BC3F3 population. A PCR product of ~150 bp (red arrow) co-segregated with the *pre2-1* mutant phenotype

mutant with the *pre1* mutation, which has been mapped to chromosome 1L using BA-translocations (Multani, Lee et al., 2003), resulted in no epistatic interaction in the F1 generation, indicating a non-allelic relationship with *pre1*. Thus, the new mutant was designated as *premature senescence2* (*pre2-1* allele). A second premature senescence mutant (Figure 1b) was also isolated from a *Mu*-active population and was found to be allelic in crosses with *pre2-1* (Figure 1c). This second allele was designated as *pre2-2*.

2.2 | Cloning and validation of the *pre2* mutation

Co-segregation analysis using a modified PCR-based Selective Amplification of Insertion Flanking Fragments (SAIFF) protocol on genomic DNA (gDNA) of eight homozygous and eight homozygous WT sibs identified a 150 bp PCR product tight linked with the mutant phenotype (Figure 1d). BLAST search using the cloned co-segregating PCR product sequence identified Zm00001d053300 (Zm-B73-REFERENCE-GRAMENE-4.0) as a putative candidate gene for the *pre2-1* allele. A *Mutator* (*Mu*) insertion in intron1, ~600 bp downstream from the exon1-intron1 junction of the gene candidate, was detected as a possible cause for the *pre2-1* phenotype. Extended linkage analysis using the gene-specific primers (GSPs) from the exon1 and exon2 of the *pre2* candidate gene in combination with a *Mu*-Terminal Inverted Repeat (*Mu*-TIR) primer established a complete linkage between the insertion and the phenotype in a population of 508 BC3F2 plants. The alignment of the FL-cDNA sequence with the genomic sequence from the public MaizeGDB confirmed that the Zm00001d053300 gene consists of 12 exons and 11 introns (Figure 2a). Since only a few partial ESTs, representing 3' end of the Zm00001d053300 gene, were found in both the public and Corteva Agriscience maize databases, we amplified and cloned ~4.0 kb full-length cDNA (FL-cDNA) by RT-PCR using two GSPs from the 5'UTR of the *pre2* candidate gene in 3'-RACE (Figure 2b). Furthermore, the *Mu*-insertion in the *pre2-1* allele resulted in four different species of mRNAs with variable expression levels in reverse transcriptase-polymerase chain reaction (RT-PCR) analysis (Figure 2c). Cloning and sequencing analysis of all four transcripts from the *pre2-1* allele and one transcript from its wild-type sib (WT sib) revealed that the smallest transcript in the mutant was exactly the same as the wild-type transcript in its WT sib (Figure S1a-i,ii). The additional three transcripts of the *pre2-1* allele were the result of splicing interference by the *Mu*-insertion in intron1. These three additional mature transcripts had an extra 122 bp sequence of the *Mu*-TIR, a 160 bp insertion comprised of 19 bp of intron1 plus 141 bp of the *Mu*-TIR, and a 373 bp insertion comprised of 232 bp of intron1 plus 141 bp of the *Mu*-TIR, respectively (Figure S1a-iii,iv,v). The extra sequences in all three mature transcripts caused frameshift and early stop codons in their predicted peptides (Figure S1b). The predicted polypeptides of the differentially spliced *pre2-1* transcripts were truncated and have only 113, 49, and 113 amino acid residues, respectively, as compared to the 1,271 amino acids in the wild type. The multiple alignments

of the mature transcripts of the *pre2-1* allele as well as of their predicted polypeptides are presented in Figures S1c.

For the candidate gene validation, we characterized the *pre2-2* allele shown in Figure 1b. However, the lack of PCR amplification for the region between exon8 and exon9 from the *pre2-2* allele as compared to its WT sib by GSPs provided us a hint for a change in the *pre2-2* allele. Southern blot analysis using the *pre2* FL-cDNA as a DNA probe detected a ~8.0 kb/*EcoRI* restriction fragment length polymorphism (RFLP) present in the *pre2-2* allele as compared to its WT sibs (Figure 2d). The ~8.0 kb/*EcoRI* fragment from the *pre2-2* allele was cloned using λ (lambda) library and sequenced to identify the cause of the *pre2-2* mutation. The partial sequence of *pre2-2* revealed an insertion of a Retro Transposable Element (RTE) belonging to the "Gypsy family" in intron8, 38 bp downstream of the exon8-intron8 junction (Figure 2a and Figure S2a). Spontaneous mutations induced by retrotransposons have been detected in various *Mutator* backgrounds (Dooner et al., 2019). Reverse genetic analysis of 412 plants, using a forward GSP from the exon8 (GSP-Exon8-F2) in combination with a reverse primer from the internal sequence of the RTE (RTE-Intron8-R1), demonstrated complete linkage between the RTE insertion in intron8 of *pre2-2* allele and the *pre2-2* mutant phenotype. These primers also allowed us to reconfirm the genotypes of the F1 allelism test by PCR fingerprinting (Figure 2e). Furthermore, expression analysis of the *pre2-2* allele by RT-PCR also revealed multiple mature transcripts (Figure 2f). The cloning and sequence analysis of the mature *pre2-2* transcripts as compared to the functional wild-type transcript of its WT sib confirmed the interference of RTE in the differential splicing of intron8. The addition of an extra ~800 bp, comprised of intron8 and RTE sequence, in the differential spliced mature transcript of the *pre2-2* mutant allele caused a frameshift leading to an early stop codon in its predicted polypeptide (Figure S2b,c). The multiple alignments of the differential spliced mature transcripts and their predicted polypeptides from the *pre2-2* allele and its WT sib are presented in Figure S2d,e, respectively. The *pre2-2* results provided further support that we have, indeed, cloned the correct gene for the *pre2* mutation. Furthermore, these results also suggest that the premature senescent phenotype in both the *pre2* alleles might be due to the production of multiple aberrant transcript variants and reduced expression of the functional wild-type transcript of the *pre2* gene.

2.3 | The expression analysis of the *ZmPre2* candidate gene

The expression of the maize *pre2* gene was compiled from more than 800 libraries developed by Corteva Agriscience using various maize tissues collected at different developmental stages, and under different biotic and abiotic stress treatments. The average gene expression of Zm00001d053300 was determined using three platforms; massively parallel signature sequencing-signature (MPSS-Sig), MPSS-Classic, and Solexa-WgT (all values in part per ten million or

PPTM) and is presented in Figure 3. The *pre2* gene is expressed in almost all maize plant tissues with maximum expression in the meristematic tissues, followed by immature ears, embryo, stalk, pericarp, roots, and leaves in both MPSS-Cla and MPSS-Sig platforms. The data demonstrate that *pre2* gene expression is enhanced under both biotic (insect infestation and disease inoculation) and abiotic (drought,

herbicide spray, and nitrate treatments) conditions (Tables S1A, S1B and S1C). For example, a maximum expression was detected in leaf whorls at the V5 growth stage upon European corn borer (ECB) infestation and in stalk after inoculation with *Colletotrichum* inoculum (Tables S1A and S1B). Similarly, the *pre2* gene expression is induced in kernels and pedicel at the R1-R2 development stage under

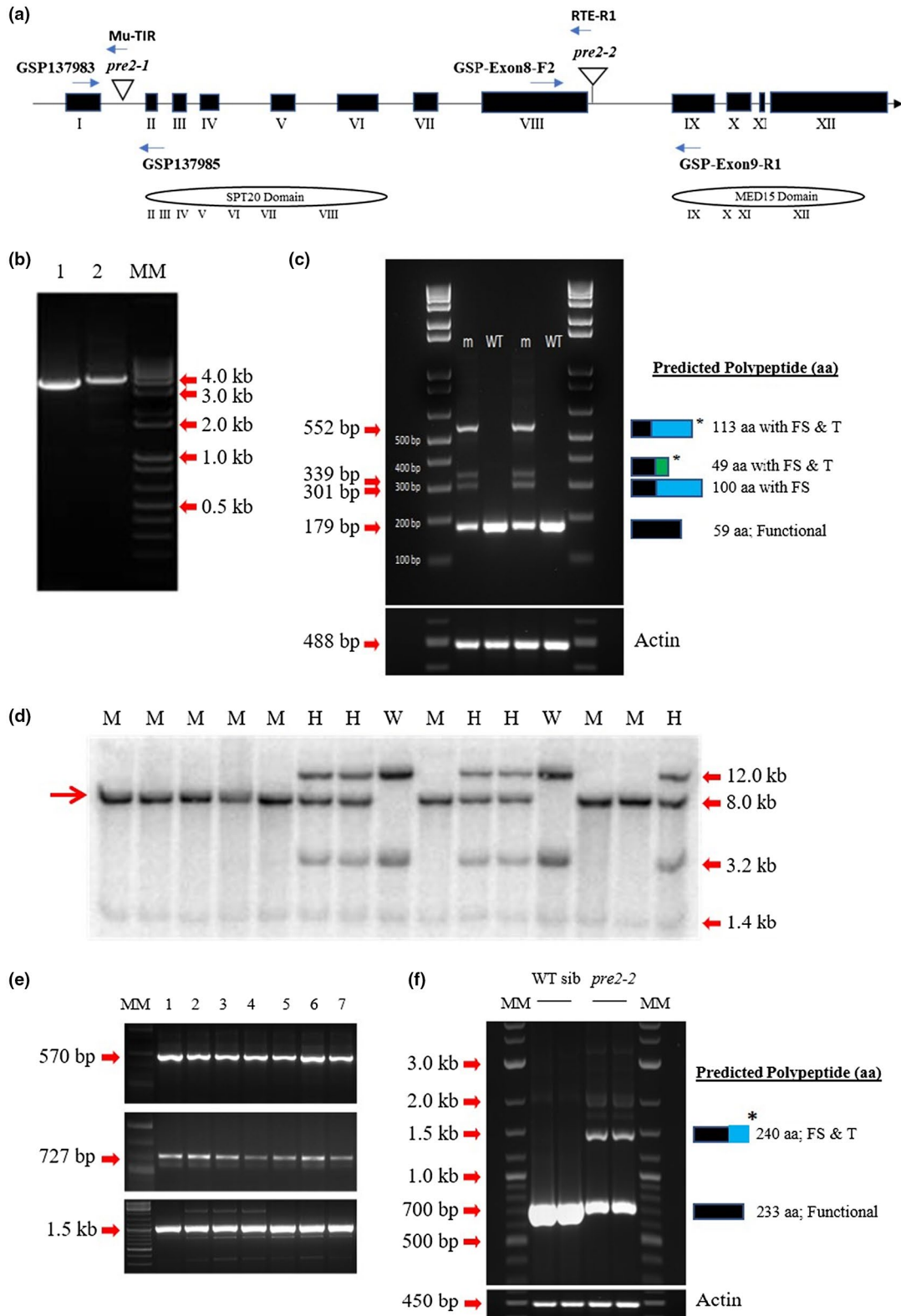


FIGURE 2 Cloning and characterization of the *Pre2* candidate gene. (a) Gene structure of the *pre2* candidate gene, Zm00001d0053300. Exons and introns are represented by filled rectangles and thin lines, respectively. Insertions of a *Mutator* (*Mu*) in intron1 and a retrotransposon (RTE) in intron8 in the *pre2-1* and *pre2-2* mutant alleles are represented by triangles, respectively. The gene-specific primers (GSPs) used in the PCR-fingerprinting and RT-PCR expression analyses are shown above the exons and arrows are pointing in their directions. (b) Full-length cDNA of *Pre2* amplified by RT-PCR using 3'-RACE. Lanes 1 and 2 are both represent the FL-cDNAs amplified by using PHN137957 and PHN137958 GSPs from the 5'-UTR of the *pre2* candidate gene. (c) RT-PCR of the *pre2-1* allele and its wild type sib using PHN137983 and PHN137985 GSPs from the exon1 and exon2 of the *pre1* candidate gene, respectively. Three additional mature transcripts of ~301 bp, ~339 bp, and ~552 bp sizes with variable intensities were detected in the *pre2-1* allele as compared to only one functional transcript of ~179 bp in its WT sib. The blue and green regions of bars on the right side of Figure 2c represent the predicted polypeptides of the differentially spliced mature transcripts resulted in frame shift (FS) and/or early termination (T) as compared to the functional predicted polypeptide represented by the black bars. Total RNA from ten days old seedlings was used in the RT-PCR analysis. (d) Southern blot (SB) analysis of a segregating population detecting an RFLP of ~8.0 Kb/*EcoRI* associated with the *pre2-2* mutant allele phenotype. The FL-cDNA was used as a DNA probe for hybridization in SB analysis. (e) PCR-fingerprinting of 7 F1 plants (lanes 2–8) of *pre2-1* and *pre2-2* allelic cross using PHN137983 in combination with *Mu*-TIR (upper lane in Figure 2e), GSP-Exon8-F2 with RTE-R1 primer (middle lane in Figure 2e), and PHN137983 with PHN137985 (lower lane in Figure 2e). (f) The RT-PCR expression analysis of the *pre2-2* mutant allele and its WT sib using GSP-Exon8-F2 and GSP-Exon9-R1 primers of the *pre2* candidate gene. Two additional mature transcripts were detected in the *pre2-2* mutant allele as compared to a functional transcript of ~700 bp size in its WT sib. The colored bars on the right side of Figure 2f are representing the predicted polypeptides as described in Figure 2c. Amplification of the *ZmActin1* was used as a control in RT-PCR analysis

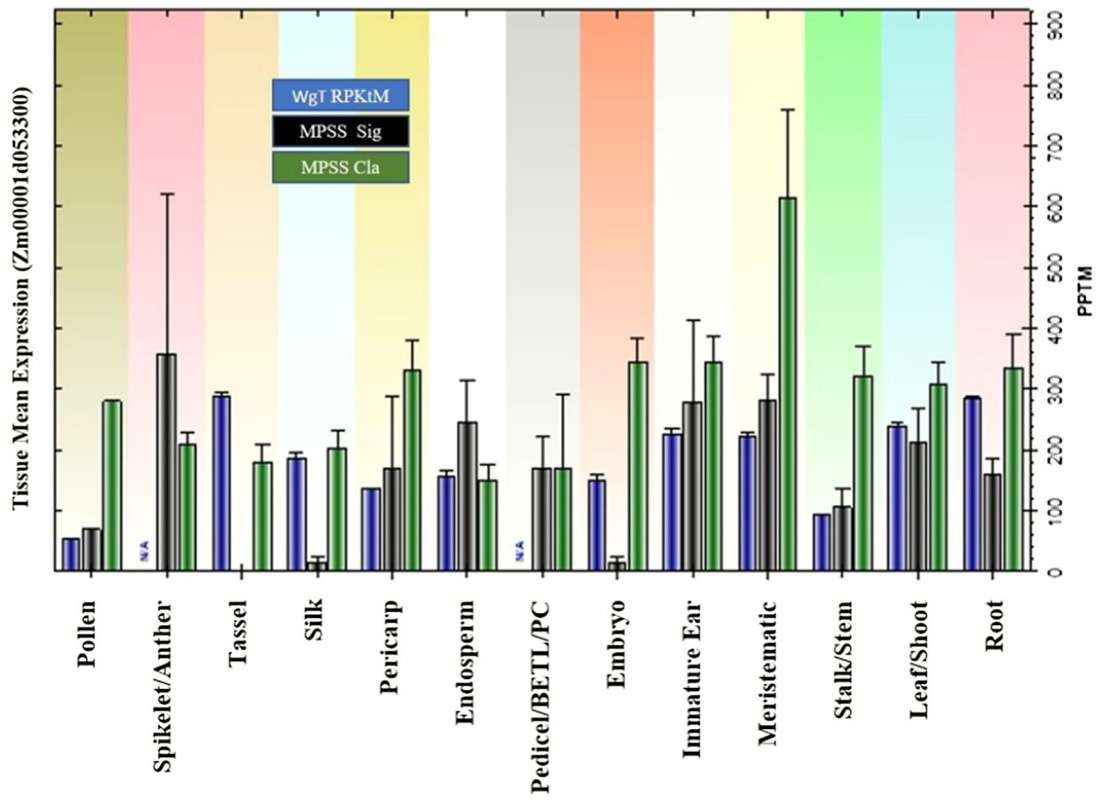


FIGURE 3 The average expression of Zm00001d053300 in different maize tissues as compiled from the Solexa-WgT (blue bars), MPSS-Signature (black bars), and MPSS-Classic (green bars) platforms of the Corteva Agriscience expression databases. The gene expression was measured in parts per ten millions (PPTM). Additional information on the tissue developmental stages and biotic and abiotic stress treatments are provided in the supplemental Tables S1A, S1B and S1C

drought stress (Tables S1A and S1B). In agreement, the eFP Atlas Browser in the MaizeGDB (https://www.maizegdb.org/gene_center/gene/Zm00001d053300) confirmed that the Zm00001d053300 gene is expressing in many tissues and enhanced in roots, leaves, and seedlings under abiotic stress (drought, salt, and temperature) and biotic stress (*Colletotrichum* and *Cercospora* infections) in the eFP Stress Browser (https://www.maizegdb.org/gene_center/gene/

Zm00001d053300#efp-stress; Hoopes et al., 2019). The expression of *ZmPre2* is induced in roots after low drought stress treatment at -0.2 MPa and severe drought stress at -0.08MPa as compared to 0MPa both after 6 and 24 hr, respectively. The *pre2* expression was reduced in mature leaves after 200 mM salt treatment (salt stress) as compared to control (0 mM), and under both heat and cold treatments as compared to their controls. The RNA-seq expression data

further confirmed that Zm00001d053300 is expressing highest (12.6 FPKM; Fragment read Per Kilobase per Million mapped reads) in leaf zone1 symmetrical samples, followed by 12.0 FPKM in ear primordium of 6–8mm sizes, and 11.3 FPKM in mature leaf 8 (https://www.maizegdb.org/gene_center/gene/GRMZM2G125342#rnaseq). The transcriptome data collected under natural leaf senescence also showed changes in the gene expression of Zm00001d053300 in the samples of both B73 and PHG35 inbred lines collected at seven different stages, starting from 9, 15, 30, 33, 36, 39, and 42 days after pollinations (Sekhon et al., 2019). Taken together, these results indicate that Zm00001d053300 is expressing in all plant tissues, and its expression is influenced by development stages as well as under environmental stimuli including temperature, light, and biotic and abiotic treatments.

2.4 | The *pre2* candidate gene is a PHYTOCHROME-DEPENDENT LATE-FLOWERING protein

The Zm00001d053300 gene is a homolog of Arabidopsis AT1G72390, which has been annotated as PHYTOCHROME-DEPENDENT LATE-FLOWERING (PHL), a nuclear receptor coactivator (source: Araport11). The BLASTP search at NCBI revealed two identifiable conserved motifs namely SPT20 (pfam12090) and MED15 (pfam09606) in the ZmPRE2 polypeptide. Based on the Gene Ontology provided by TAIR (The Arabidopsis Information Resource), this peptide has been assigned a biological process involved in the regulation of transcription by RNA Polymerase II (GO: 0008150). The ISM (Inferred from Sequence Model) identified GO: 0005886 associated with a component of the SAGA complex, located in the plasma membrane and expressed during the growth and developmental stages of the plant (Arabidopsis Atlas eFP Browser at <http://www.bar.utoronto.ca/>). The PRE2 polypeptide contains transcription factor Spt20 (173 bp–3,799 bp), InterPro domain (IPRO21950), which is found in the Spt20 family of proteins from both human and yeast. The SPT20 protein is part of the SAGA (Spt-Ada-Gcn acetyltransferase) complex. The SAGA complex is a multiprotein complex that possesses histone acetyltransferase activity. The PRE2 polypeptide is 1,271 amino acids (aa) long as compared to 1,325 aa in Arabidopsis and 1,319 aa in sorghum. Proteomics data associated with ZEAMMB73_993122 (GRAMENE ID: GRMZM2G125342) showed a small domain of 14 amino acids (APTGPV**IQ**SPVSSK) as phosphorylated peptide and Serine (underlined bold aa) as a phosphorylation site. The deduced amino acid sequence of the maize ZmPRE2 polypeptide was aligned with homologous polypeptides of both monocot and dicot plant species and presented in Figure S3a. The multiple alignment of the PRE2 polypeptides showed that all plants contain the SPT20 conserved motif. Among monocots, the PRE2 polypeptides of sorghum (*Sorghum bicolor*) and Bahia grass (*Paspalum notatum*) were found to be 87.2% and 90% identical with maize at amino acid level, respectively, whereas the rice (*Oryza sativa*), barley (*Hordeum vulgare*), and Brachypodium (*Brachypodium*

distachyon) polypeptides have diverged from maize and showed only 68%, 65.3%, and 68.4% identity, respectively. Homologs in dicots including Arabidopsis (*Arabidopsis thaliana*), soybean (*Glycine max*), and potato (*Solanum tuberosum*) showed 34%, 36%, and 33% identity with the ZmPRE2 polypeptide at the global alignment level, respectively (Figure S3a). Despite the overall sequence divergence along the full-length of the PRE2 polypeptides across a variety of plant species, molecular analysis revealed five conserved domains in the SAGA complex (underlined and highlighted in yellow in Figure S3a). These five highly conserved domains are variable in lengths, ranging from 15 to 46 aa. Their consensus sequences, along with a subset of variable amino acids (X) representing the most common amino acids within a conserved domain across species are presented in Figure S3b. The phylogenetic relationship among the selected monocot and dicot plant species by their full-length polypeptide sequences is presented in Figure S3c, indicating the divergence of polypeptides between the monocots and dicots.

The second conserved motifs in the ZmPRE2 polypeptide near the C-terminus is MED15 (pfam09606). MED15 is a PCQAP PC2 (*positive cofactor2, multiprotein complex*; NCBI database Gene ID: 51586) glutamine/Q-rich-associated protein associated with the mediator complex involved in RNA polymerase II-dependent transcription. Three domains with Q-rich motifs have been detected in the ZmPRE2 polypeptide, but the third polyQ tract near the C-terminus is 41–70 aa long and is highly conserved in all plant species (Figure S3a), indicating that it might be playing an essential role in the function of the polypeptide. The predicted polypeptides of the differentially spliced mature transcripts in both the *pre2* alleles lacked this MED15 motif either by modifying or truncating the amino acid sequence due to frameshift and early termination codon (Figure S2d,e).

2.5 | Overexpression and downregulation of endogenous *ZmPre2* mRNA in FASTCORN

For transgenic studies, the *ZmPre2* RNAi suppression and overexpression (Ox) constructs were transformed into a fast cycling maize line (FASTCORN). All 10 events in RNAi construct (PHP43211) and 8 of 10 events of the Ox construct (PHP43209) were single copy. The relative gene expression in 5 out of 10 RNAi events was significantly low (ranging from 0.07 to 0.554) as compared to internal transgenic and non-transgenic controls (Table 1). All but one overexpression events had 2x more relative expression ranging from 2.171 to 2.918. Three RNAi events (EA2850.045.1.4, EA2850.045.1.5, and EA2850.045.2.5) were found to have significantly higher ear length, ear width, and total seed numbers in T0 generation (Table 1; Figure 4), which might be associated with their relative gene expressions. The premature senescence phenotype was not observed in these events as all 10 T0 RNAi events were heterozygous and the recessive mutant phenotype would not express in T0 generation. However, we might have missed the segregation of the phenotype

TABLE 1 The data analysis of 10 T0 events each of PHP43211 and PHP43209 representing RNAi and Over Expressed constructs, respectively. Plus (+) and minus (-) signs in front of the mean illustrate the percentage of a trait was increased or decreased for transgene over the null, respectively. Colors representation: Green (positive changes with p value $\leq .1$); Red (negative changes with p value $\leq .1$); and Blue color represents a significant p value

Event name	Ear Length (cm)		Ear Width (cm)		Max Total Plant Area		Seed Number		Stay Green		Rel. Exp.	Copy No.
	Data	Z Score	Data	Z Score	Data	Z Score	Data	Z Score	Data	Z Score		
PHP43211												
EA2850.045.1.1	10.354	0.170	3.632	1.850	727,206	2.700	175	0.710	0.142	0.130	0.554	1
EA2850.045.1.2	9.205	-0.77	3.139	-0.13	380,383	-1.38	114	-0.99	0.1536	0.81	-0.21	1
EA2850.045.1.3	10.693	0.45	3.144	-0.11	604,991	1.26	145	-0.12	0.1306	-0.54	-0.169	1
EA2850.045.1.4	12.814	2.17	3.55	1.52	628,505	1.54	224	2.09	0.1562	0.97	0.337	1
EA2850.045.1.5	11.501	1.1	3.614	1.77	766,178	3.16	212	1.75	0.1394	-0.02	0.398	1
EA2850.045.2.1	8.415	-1.41	3.063	-0.43	417,310	-0.94	106	-1.21	0.1247	-0.89	-0.527	1
EA2850.045.2.2	9.281	-0.71	2.784	-1.55	320,819	-2.08	102	-1.33	0.1293	-0.62	0.07	1
EA2850.045.2.3	5.624	-3.69	2.768	-1.61	344,943	-1.8	20	-3.62	0.1054	-2.02	-0.091	1
EA2850.045.2.4					237,595	-3.06			0.2214	4.8	-2.77	1
EA2850.045.2.5	12.457	1.88	3.544	1.49	407,197	-1.06	228	2.2	0.1449	0.3	0.275	1
PHP43209												
EA2850.009.1.1	8.018	0.020	3.102	-0.210	662,691	1.160	94	-0.140	0.094	-1.310	2.236	1
EA2850.009.1.2	7.684	-0.18	3.266	0.58	634,324	1	83	-0.47	0.0983	-1.12	2.504	1
EA2850.009.1.3	7.284	-0.42	3.119	-0.12	637,720	1.02	90	-0.26	0.0955	-1.23	-0.741	1
EA2850.009.1.4	7.106	-0.52	2.969	-0.85	569,212	0.61	81	-0.53	0.1124	-0.57	2.447	2
EA2850.009.1.5	10.123	1.28	3.373	1.1	604,352	0.82	132	1.01	0.0954	-1.24	2.191	1
EA2850.009.2.1					70,953	-2.34			0.1614	1.37	2.805	2
EA2850.009.2.2	9.888	1.14	3.076	-0.33	619,971	0.91	110	0.34	0.1181	-0.34	2.171	1
EA2850.009.2.3	8.638	0.3	3.104	-0.2	559,924	0.56	112	0.4	0.103	-0.94	2.918	1
EA2850.009.2.4					104,745	-2.14			0.1587	1.27	2.897	1
EA2850.009.2.5	7.953	-0.02	3.093	-0.25	479,917	0.08	98	-0.02	0.1146	-0.48	2.201	1

in the T1 generation because we characterized only three outperforming events under different sets of experimental conditions (see below). None of the single-copy overexpression events out yielded the null WT controls. Rather, two overexpression events (EA2850.009.2.1 and EA2850.009.2.4) with high relative expression (2.805 and 2.897) had negative Z scores for maximum total plant area and developed no ears on the plants (Table 1). Moreover, the three selected RNAi events (EA2850.045.1.4, EA2850.045.1.5, and EA2850.045.2.5) also had higher biomass as compared to all overexpression events (Table 1) and its own null WT sibs. These three RNAi events were used for conducting NUE reproductive assay in T1 generation under 4.0mmol Nitrate-suboptimal nitrogen conditions (Table 2). Two of three events (EA2850.045.1.5 and EA2850.045.2.5) showed a significant increase (per cent change vs. Null) for silk count, ear length, ear width, and ear area (Table 2). In addition to these traits, event EA2850.045.2.5 also showed a significant difference for days to shed and days to silk as compared to its nulls. Taken together these results indicate that the downregulation of the *Pre2* gene expression might be useful for improving agronomic traits.

2.6 | Molecular characterization of the *pre2* homolog in Arabidopsis

Three independent T-DNA insertional alleles (SALK_017615, SALK_079273, and SALK_107247) were identified in At1G72390 from the Arabidopsis database using the *ZmPre2* gene sequence as a query. Seed of these mutant lines was obtained from the Arabidopsis Biological Resource Center (ABRC, <https://abrc.osu.edu/>) and characterized for T-DNA insertions sites by PCR-genotyping using various GSPs in combination with T-DNA primer (P1052). Since both the SALK_079273 and SALK_107247 lines had T-DNA insertions in the 3' UTR region of the candidate gene (Figure S4a), we focused only on the SALK_017615 line where the T-DNA is inserted in the coding sequence. The SALK_017615 mutant line is exactly the same mutant allele characterized as a late-flowering mutation and designated as *phl* mutant in Endo et al. (2013) study. The PCR amplification of the T-DNA flanking sequence using a GSP (P1233) in combination with T-DNA primer (P1052) confirmed that the T-DNA insertion is present in exon10 of the At1G72390 gene (Figure S4a) and all plants had the T-DNA insertion (Figure S4b, panel 1 from

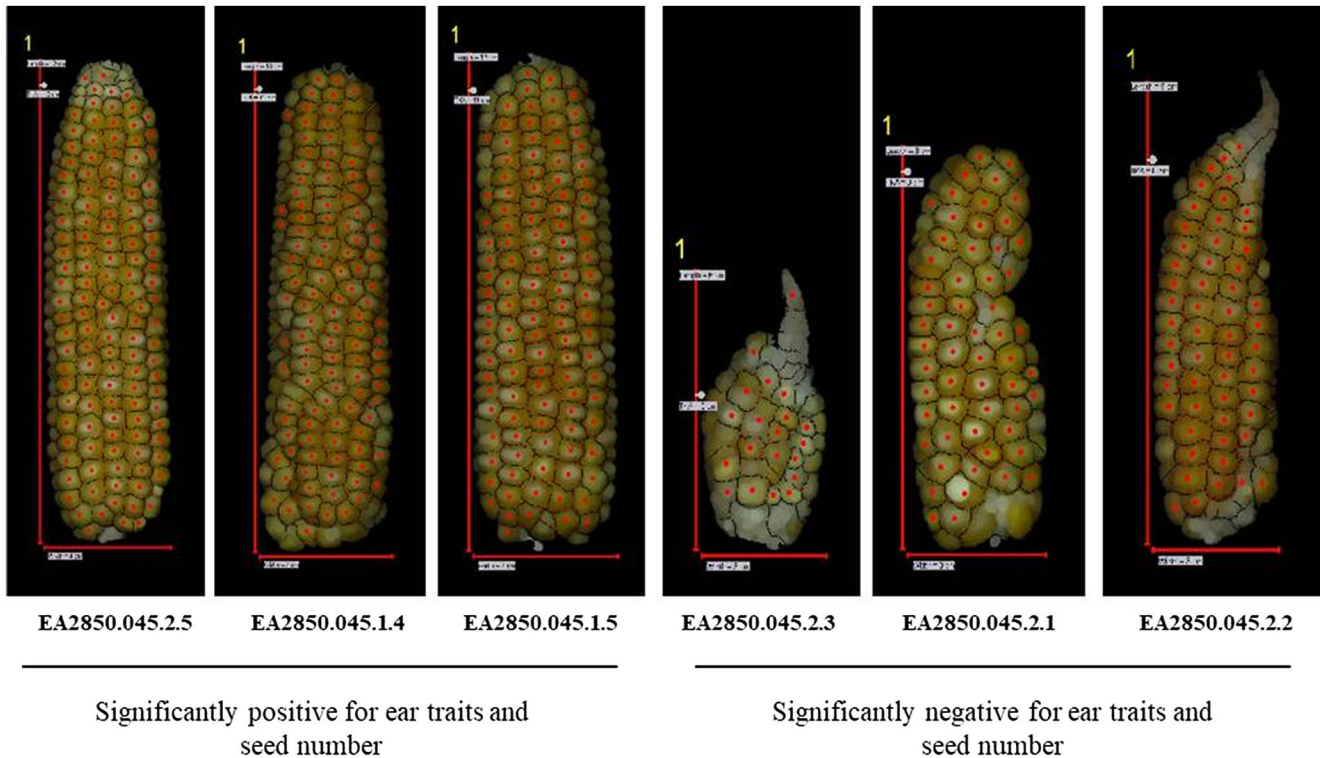


FIGURE 4 Phenotypic data on ear traits captured through Ear Photometry on T0 events in RNAi construct (PHP43211). First three events significantly positive for ear traits were characterized in NUE reproductive assay using suboptimal Nitrogen treatment (4.0 mmol Nitrate) in T1 generation (See Table 2)

top). The use of two GSPs (P1233 and P1234), flanking the T-DNA insertion site, amplified the DNA region only from the wild-type allele. The expected PCR products were present in all plants with the exception of plants # 11 and # 25 (Figure S4b, panel 2 from top), indicating that all plants except # 11 and # 25 were heterozygous for the insertion. Furthermore, the PCR-genotyping was repeated on 256 plants of a self-progeny of a heterozygous plant. The segregation ratio of 62:131: 63 for homozygous mutant, heterozygous WT sibs, and homozygous WT, respectively, fits well in 1:2:1 ratio ($\chi^2 = 0.148$) confirmed that the mutant phenotype is controlled by a single recessive locus. Based on the genotyping results, plants # 11 and # 25 were identified as homozygous for T-DNA insertions. The At1G72390 gene is expressing at a low level in almost all plant parts with the exception of siliques and maturing seeds (Arabidopsis eFP Browser at <http://www.bar.utoronto.ca/>). The PHL gene expression was reduced 50-fold in the *phl* mutant as compared to its WT sib (Endo et al., 2013). Seed of the homozygous mutants and homozygous WT sibs was increased for further morphological, drought, and NUE characterizations. Morphological trait data of homozygous knockout plants # 11 and # 25 (*AtPre2*-KO) were compared with their homozygous WT (+/+) and heterozygous WT sib (+/*AtPre2*-KO) plants at flowering. Both homozygous mutants were robust in growth with more pods but were 4 to 5 days late in flowering and maturity as compared to its WT sibs (Figure 5a). For measuring total biomass, nine plants each of knockout # 11, knockout # 25, homozygous WT sibs, and heterozygous WT sibs, were

harvested and air-dried for 14 days at room temperature. The total biomass of both knockouts (combined) was significantly higher (t test at $p \leq .01$) when compared to both homozygous and heterozygous WT sibs (Figure 5b).

2.7 | Drought tolerance assay of T-DNA knockouts and *ZmPre2* over-expressed transgenes in Arabidopsis

We simulated drought conditions by giving plants no water over a period of time, and evaluated drought tolerance by looking for differences in physiological and/or physical condition, including (but not limited to) vigor, growth, size, or root length, or in particular, leaf color, and leaf area size. The *AtPre2*-KO mutant plants showed clear visual differences after giving water stress for 4 days (day 9 to day 12; Figure 5c) and also showed a positive score greater than 0.9 with positive standard deviation in 72 plants in all eight flats tested for each mutant compared to their respective WT sibs (Figure 5d). The data demonstrated that the *AtPre2*-KO mutant plants significantly outperformed their wild-type sib controls. The second control used in this experiment was *ZmPre2* gene overexpressed under 35S promoter in Arabidopsis. The Ox transgene plants showed a moderate 2-sigma score, but with negative standard deviation, indicating a hypersensitivity to drought stress (Figure 5d), thus, further authenticating the drought assay results.



TABLE 2 Event variable summary using two-tailed *p*-value: Characterization of three selected RNAi (PHP43211 construct) events in NUE reproductive assay using suboptimal Nitrogen treatment (4.0 mmol Nitrate) in T1 generation. Plus (+) and minus (-) signs in front of the mean illustrate the percentage a trait increased or decreased for transgene over the null, respectively. Colors representation: Green (positive changes with *p* value $\leq .1$); Red (negative changes with *p* value $\leq .1$); and Blue color represents a significant *p* value. The relative chlorophyll content was measured by CCM-200 in CCI units (Chlorophyll Content Index; see M & M for detail). The data on ear traits were captured by imaging 8 days after self-pollination (8DAS)

Event name	CCI		Days to shed		Days to silk		Silk count 8DAS		Ear area 8DAS (sq. cm)		Ear length 8DAS (cm)		Ear width 8DAS (cm)	
	<i>p</i> -value	% chg. vs. Null	<i>p</i> -value	% chg. vs. Null	<i>p</i> -value	% chg. vs. Null	<i>p</i> -value	% chg. vs. Null						
EA2850.045.1.4	.383	-6.20%	.385	-0.70%	.245	.245	.051	-11.90%	.204	-7.80%	.276	.276	.064	-5.40%
EA2850.045.1.5	.809	1.80%	.248	1.00%	.351	1.80%	.101	10.50%	.062	11.70%	.073	.073	.576	1.60%
EA2850.045.2.5	.989	0	0	11.20%	0	11.20%	.174	0	0	0	.004	.004	.132	4.50%

2.8 | Evaluation of *AtPre2*-KO mutant on low and high nitrogen

For Low N plate assays, 32 mutant and 32 wild-type plants were grown on square plates in Low N medium. On day 12 (9 days of growth), seedling status was evaluated by imaging the entire plate for total rosette area (Figure S5) and the percentage of color that falls into a green color bin using hue saturation and intensity data (HSI). Total rosette area was used as a measure of plant biomass, whereas the green color bin (Bin2 Fraction) was shown by dose-response studies to be an indicator of nitrogen assimilation. In Low N assay, the *AtPre2*-KO mutant plants showed a significantly higher average total area and green color (Figure 6a). For high Nitrogen (High N) root assays, 16 mutants and 16 wild-type plants instead of 32 each were grown on plates in the same light and temperature conditions as described above. The plates had the same medium except it was containing 60 mM of potassium nitrate. Total root biomass was measured by imaging in pixels (Figure S6) and the experiments were repeated four times. The analysis of the scatterplot data (Figure S7) revealed that in each replication mutant plants were hypersensitive to higher concentration of N leading to severe root growth inhibition as compared to its wild-type sib plants (Figure 6b).

2.9 | *AtPre2*-KO mutant showed hypersensitivity to ABA

To elucidate the function of the *AtPre2* protein in drought tolerance, ABA sensitivity assay was conducted. The *AtPre2*-KO mutant showed hypersensitive response to 1 μ M ABA concentration in multiple times repeated the experiment. The seed germination in the mutant was reduced or delayed by more than 50% as compared to Col-0 WT in the presence of 1 μ M ABA (Figure 6c). Searches of the public expression databases revealed that the endogenous gene expression of the *At1G72390* in wild-type plants was higher in guard cells, and downregulated by ABA treatment both in seedling and leaf (Arabidopsis eFP Browser at <http://www.bar.utoronto.ca/>).

3 | DISCUSSION

A recessive mutant exhibiting a premature senescence phenotype during flowering initiation was isolated from the *Mu*-active materials. Based on its non-allelic relationship with the existing *pre1* mutation (Multani, Lee et al., 2003) and mapping to chromosome 4, it was designated *pre2-1*. A candidate gene for the *pre2-1* mutation was isolated using a PCR-based co-segregation SAIFF protocol (Jiao et al., 2019; Muszynski et al., 2006). The BLAST search using the sequence of the co-segregating PCR product identified the GRMZM2G125342 (B73 RefGen_v3) or Zm00001d053300 (Zm-B73-REFERENCE-GRAMENE-4.0) in the MaizeGDB as a putative candidate gene for the *pre2-1* mutation. The Zm00001d053300 is a homolog of the Arabidopsis *AT1G72390* gene, which has been characterized earlier

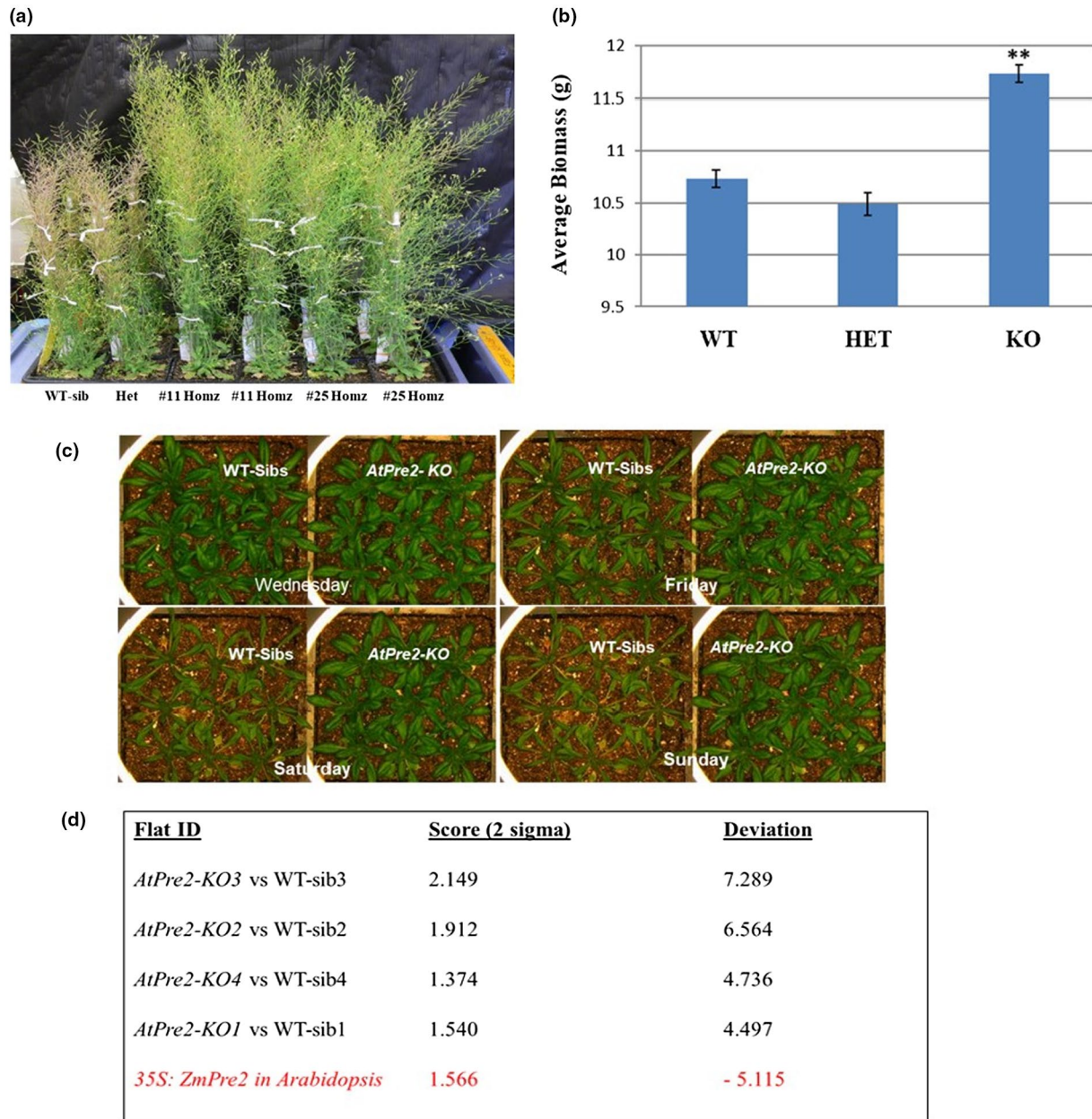


FIGURE 5 Phenotypic characterization of the homozygous *AtPre2-KO* mutant under normal and drought stress assay. (a) Two rows each of the homozygous mutant lines (# 11 and # 25) showing robust growth with more pod numbers but late in flowering and maturity by 4–5 days as compared to their heterozygous and homozygous WT sibs in repeated experiments. (b) The knockout mutant showed a significantly higher average biomass (**t test at $p \leq .01$) under normal growth conditions. (c) The *Atpre2-KO* mutant plants did not show stress symptoms after water withdrawal as compared to its WT sib. Only two representative pots are shown above, but all 16 pots (144 plants in 4 flats) for each of the KO and their WT sibs in this experiment showed similar results. (d) The *AtPre2-KO* plants in all 4 flats showed positive scores [A score (2 sigma) greater than 0.9 with positive standard deviation is considered an outlier in this assay] demonstrating that the mutant plants outperformed significantly better than their WT sibs used as control. The *Arabidopsis* transgene plants overexpressing (Ox) the *ZmPre2* gene under 35S promoter (35S:*ZmPre2*-Ox) showed hypersensitivity to drought [A score (2 sigma) with negative deviation]

and found to accelerate flowering through physical interactions with phytochrome B and CONSTANS (Endo et al., 2013). Insertion of a *Mutator* in intron1 of the candidate gene was a possible cause for the *pre2-1* mutant phenotype. The candidate gene was independently validated by characterizing another allele, *pre2-2*, which was also isolated from a *Mu*-active population. The extended linkage and

RT-PCR expression analyses of both the *pre2-1* and *pre2-2* alleles established that transposable elements appear responsible for the production of aberrantly spliced transcripts. The presence of multiple transcript variants in addition to the functional transcript of the *pre2* gene in both alleles clearly indicated that both *pre2* alleles were not null. Furthermore, the presence of a functional mature transcript

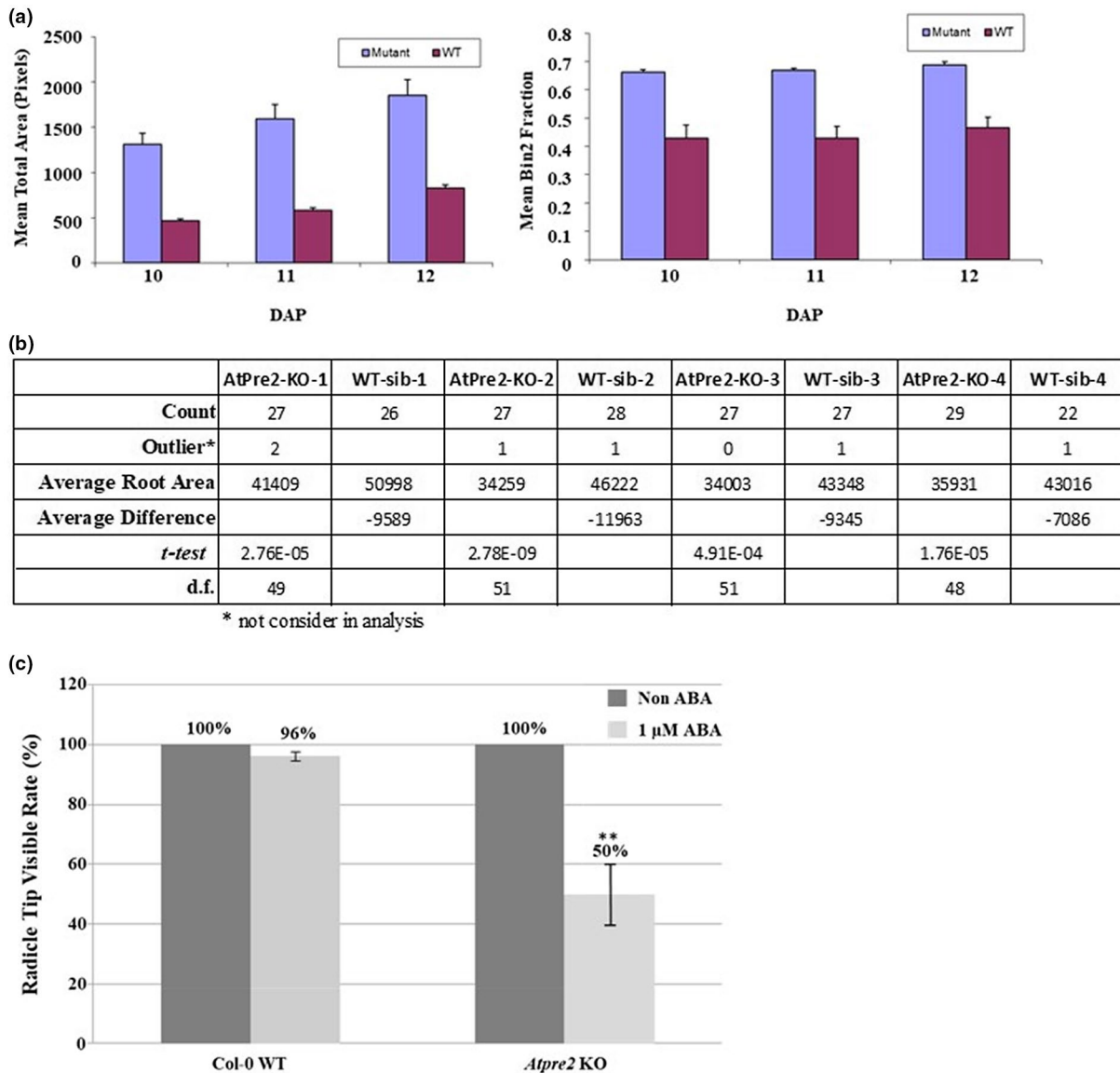


FIGURE 6 Characterization of the *AtPre2*-KO mutant in low Nitrogen (Low N) and high Nitrogen (High N) assays. (a) The average plant size of the rosette (Mean Total Area in Pixels) and Color (Mean Bin2 Fraction) in mutants was significantly higher as compared to their respective WT sib controls at 10, 11, 12 days after planting (DAP) in Low N assay. (b) Analysis of the scatterplot data collected on root area in the *AtPre2*-KO and its WT sibs measured in pixels per plant (Scatterplot shown in Figure S7) screened in High N assay. The *t* test values confirmed that the *AtPre2*-KO mutants are more sensitive to root inhibition at High N as compared to their WT sib controls. (c) Seed germination rate of the *AtPre2*-KO mutant under ABA treatment. The *AtPre2*-KO mutant showed hypersensitive response to 1 μ M ABA and germination rate was reduced significantly (50%) compared to 100% in Col-0 WT control used in this experiment

in both *pre2* alleles might be adequate for development during early growth stages, but the expression of the functional *pre2* gene may not be sufficient for normal development during later growth stages or under changing environmental conditions in the field. Taken together, these results suggest that we have cloned the correct gene responsible for the *pre2* mutant phenotype in maize, which might be due to the presence of multiple variants of the mature mRNAs of the *pre2* gene in both the *pre2* alleles. We could not validate the cross-species *pre2*-phenotype as the transgenic *Arabidopsis* plants overexpressing the *Zmpre2* gene were hypersensitive and died in drought stress assay.

A detailed expression analysis from the Corteva Agriscience and public databases showed that Zm00001d053300 is expressed at fairly constant levels in most plant tissues starting from early development. It is also evident that the expression of Zm00001d053300 is influenced by both biotic (disease infection and insect infestations) and abiotic (drought, salt, temperature) stresses. Furthermore, the changes detected in the average expression of Zm00001d053300 in leaf transcriptomic datasets post-pollinations samples also indicate that the gene expression is influenced by normal leaf senescence post-flowering in both B73 and PHG35 inbred lines (Sekhon et al., 2019). The higher expression level of Zm00001d053300 in leaves post-pollination



supports the fact that an optimum threshold of the wildtype transcript is required for normal function at any development stage. Thus, the *pre2* phenotype observed in both mutant alleles maybe due to insufficient wildtype transcript at the pre-flowering stage.

The ZmPRE2 polypeptide has two identifiable conserved motifs namely SPT20 and MED15. The SPT20 protein is a module of the SAGA (Spt-Ada-Gcn5 acetyltransferase) transcription coactivator complex. The SAGA complex is a 2MDa multi-protein chromatin-modifying complex that is conserved between yeast and humans, harboring two known enzymatic modules that mediate the acetylation and de-ubiquitination of histones and non-histone substrates (Koutelou et al., 2010). The yeast SAGA complex is thought to control transcription of approximately 10% of genes, particularly stress-related genes (Lee et al., 2000). One of the central questions in eukaryotic transcription is how activators can transmit their signal to stimulate gene expression in the context of chromatin. The multi-subunit SAGA coactivator complex has both histone acetyltransferase and de-ubiquitination activities and remodels chromatin to allow transcription (Moraga & Aquea, 2015). Where and how the SAGA complex is able to regulate transcription at specific loci is poorly understood. Using mass spectrometry, immunoprecipitation, and Western blot analysis Nagy and his colleagues (Nagy et al., 2009) identified human SPT20 (hSPT20) as the human homolog of the yeast Spt20 and showed that hSPT20 is a bona fide subunit of the human SAGA (hSAGA; previously called TFIIIC/STAGA/PCAF) complex and that hSPT20 is required for the integrity of the hSAGA complex. They demonstrated that hSPT20 and other hSAGA subunits, together with RNA polymerase II, are specifically recruited to genes induced by endoplasmic reticulum (ER) stress. In good agreement with the recruitment of hSAGA to the ER stress-regulated genes, knockdown of hSPT20 hampers ER stress response. Surprisingly, hSPT20 recruitment was not observed for genes induced by another type of stress. These results provide evidence for a direct and specific role of the hSPT20-containing SAGA complex in the transcriptional induction of ER stress-responsive genes. Thus, hSAGA regulates the transcription of stress-responsive genes in a stress type-dependent manner. In yeast, deletions of the SAGA acetyltransferase subunit exhibited increased leucine uptake which was dependent on the expression of an amino acid permease (Takahashi et al., 2012). The regulation of nutrient uptake as a physiological function for the SAGA complex provides a potential link between cellular metabolism and chromatin regulation.

The second conserved motif MED15 is a general transcriptional cofactor of the mediator complex involved in RNA polymerase II-dependent transcription, originally called Gal11 and Spt13 and found in yeast as an essential factor for Gal4-dependent transactivation (Fassler & Winston, 1989; Suzuki et al., 1988). The Mediator complex is composed of at least 31 subunits: MED1 to MED31. The subunits form at least three structurally distinct submodules. The head and the middle modules interact directly with RNA polymerase II, whereas the elongated tail module interacts with gene-specific regulatory proteins. The MED15 belongs to the tail module and might be playing a role by interacts with gene-specific

regulatory proteins. As many as 45 proteins, that interact with the AtMed15a KIX domain, including 11 TFs, 3 single-strand nucleic acid-binding proteins, and 1 splicing factor, have been detected (Kumar et al., 2018). Most of these transcription factors share the transactivation domain, 9aaTAD, which directly interacts with the KIX domain of the MED15 (Piskacek et al., 2007). MED15 gene contains stretches of trinucleotide CAG repeats in the mature transcript and coding glutamine (Q). The PRE2 polypeptide has three conserved regions with stretches of polyQ amino acids and the third domain located near the C-terminus, which is 41–60 aa long and highly conserved in all plant species. We speculate that the function of the Zm00001d053300 gene might have diverged in maize as compared to Arabidopsis due to divergence in the amino acid sequence or changed due to shorter tract polyQ at the C-terminus of its polypeptide as compared to Arabidopsis. The polyQ sequences have been found to facilitate protein/protein interactions and alteration of this important biological function results in the gain of abnormal interactions in humans (Schaefer et al., 2012). Furthermore, the Q-rich (QR) regions present in yeast transcription factors were found to be engaged in efficiently binding and localization to the plasma membrane (Sen et al., 2017). Thus, failure of the PHL to form sufficient interactions with other proteins, or localization of PHL to the correct compartment (nucleus), might be the ultimate cause of the premature senescent phenotype. Although the general role of the SAGA complex is conserved in eukaryotes, that role may have diverged in plants and further between monocots and dicots as evidenced by sequence divergence. In both species, the lack of the polyQ tract in mutant alleles likely reflects a key role in the functioning of the complex. However, the short lifecycle of Arabidopsis (and FASTCORN) and non-parallel mutant phenotype may reflect a subspecialization or increased requirement for the coactivator complex in naturally senescing maize leaves under natural light conditions.

The Spt20, the recruiting module, is conserved in several photosynthetic organisms (Srivastava et al., 2015) and in Arabidopsis, an SPT20 domain-containing protein has been reported as an interactor that bridges PHYTOCHROME B (phyB) and CONSTANS (CO) protein involved in the photoperiodic regulation of flowering (Endo et al., 2013). In agreement, the biomass and seed yield increase reported here in the *Atpre2-KO* might be due to late flowering and delay maturity trait. It is documented that some of these SPT20 proteins are likely involved in the regulation of the inducible expression of genes under light, cold, drought, salt, and iron stress (Moraga & Aquea, 2015). Plants sense environmental stimuli such as light to regulate their flowering time. The disappearance of fluorescence of PHL-YFP or PHL-GUS fusion protein expressed under 35S or PHL promoters after 4-hr treatment of white light indicates light-dependent destabilization of PHL in Arabidopsis (Endo et al., 2014). The lack of expression of the premature senescent phenotype in the FASTCORN RNAi transgene study might be due to the shorter developmental lifecycle (60 days instead of 100) or altered light quality (less UV) under greenhouse conditions. Plants have developed sophisticated signaling pathways that act in concert to counteract



salinity and drought stress conditions through the action of transcription factors and histone modifications, thereby promoting the induction of many stress-responsive genes and ultimately increasing stress tolerance (Golldack et al., 2014). Our results confirmed these additional roles to the PHL protein under abiotic stresses. The overexpressing transgenes with greater than 2x expression in maize and the overexpression of the maize *pre2* gene in Arabidopsis under 35S promoter resulted in hypersensitivity under drought stress, whereas the downregulation of the *pre2* candidate gene by RNAi improved agronomic performance under both drought and nitrogen stress conditions. These observations indicate that reduction in gene expression of Zm00001d053300 enhanced the ability of the transgene plants to withstand against both water stress and sub-optimal nitrogen at flowering. To validate the function of the Zm00001d053300 gene across species, we studied a T-DNA knockout of Arabidopsis (SALK_017615) for phenotypic characterization under abiotic conditions. Since the SALK_017615 was also characterized by Endo and colleagues for late flowering, thus, the *AtPre2-KO* mutant used in this investigation and *phl* mutant are synonyms. The *AtPre2-KO (phl)* with 50-fold reduced transcript (Endo et al., 2013) outperformed its WT sib controls under both drought stress and Low N conditions, thus, validated the involvement of the *pre2* candidate gene in drought and nitrogen response pathways.

ABA has long been regarded as a positive regulator of leaf senescence. Loss-of-function mutants in the Arabidopsis *receptor protein kinase1 (RPK1)* were significantly delayed in age-dependent senescence, and mutants exhibited reduced sensitivity to ABA-induced senescence (Lee et al., 2011). In the present study, the *AtPre2-KO* showed hypersensitive response to ABA and reduced seed germination. However, in the public database endogenous expression of the PHL gene is downregulated in guard cells by ABA treatment, both in seedlings and leaves, and upregulated by nitrate in roots. These results indicate that the PHL might be playing a direct or indirect role in ABA and N signaling/pathways.

In summary, the present investigation has assigned additional functions in both maize and Arabidopsis PHL proteins by demonstrating that the modulation of the endogenous gene expression of PHL (Zm00001d053300) resulted either in hypersensitivity, or enhanced performance under abiotic stress. Thus, the expression of the PHL gene can be manipulated in crop plants for drought and/or NUE improvement. It is our opinion that additional experiments are needed to understand the mechanisms by which the downregulation of endogenous PHL expression is contributing to drought tolerance, and making plants more efficient in nitrogen utilization, before exploiting this gene for a commercial product.

4 | MATERIALS AND METHODS

4.1 | Plant materials

A *premature senescence* mutant was isolated from public *Mu*-active lines crossed with a Pioneer Brand elite non-stiff stalk (NSS) inbred

line. The resulting F1 was crossed again with the same recurrent parent and the BC1F1 was self-pollinated to develop a BC1F2 population. BC1F2 families segregating for the premature senescing mutant phenotype were used to select mutant and advanced to BC2F1 by backcrossing. This process was repeated to develop a BC3F2 population which was subjected to the rough mapping of the *premature senescence* mutation using 4K Illumina markers. Based on the mapping results and reciprocal allelic crosses with *pre1* (which had been mapped to chromosome 1L by Multani, Lee et al. (2003), it was designated *pre2* mutation (*pre2-1* mutant allele). After cloning a candidate gene for the *pre2* mutation, extended linkage analysis was performed by genotypic and phenotypic characterizations of 508 BC3F2 plants using GSPs in combination with a *Mu*-TIR primer. The *pre2-1* mutant was advanced to BC7 generation by crossing with the same recurrent parent and genotyping in each generation. The homozygous *pre2-1* mutant and its homozygous WT sib from BC7F2 generation were used in RT-PCR analysis. A second mutation was also isolated from our internal *Mu*-active collection and found to be allelic to *pre2-1* and designated *pre2-2*.

4.2 | Candidate gene isolation and validation for the *pre2* mutation in maize

The genomic DNA of eight homozygous *pre2-1* mutants and eight homozygous WT sibs (+/+) from BC3F3 were subjected to co-segregation analysis. To identify the candidate gene responsible for the *pre2* phenotype, we used a modified PCR-based SAIFF protocol (Jiao et al., 2019; Muszynski et al., 2006). The co-segregated PCR-amplified product was excised from the gel, cloned in TA cloning vector, and sequenced using M13F and M13R primers. The *Mu*-flanking sequence of the co-segregating PCR-amplified product (after truncating the *Mu*-TIR sequence), was used as a query in BLAST search to identify the candidate gene and *Mu*-insertion site in the candidate gene sequence. The GSPs were designed from the candidate gene and used in combination with a *Mu*-TIR primer to establish a tight linkage between the candidate gene and the *pre2* mutant phenotype. The *pre2-2* allele was subjected to reverse genetics using GSPs and the *Mu*-TIR primers, Southern blot analysis, and restriction map of the candidate gene sequence to narrow down the region having change responsible for the *pre2-2* phenotype. The 8.0Kb/*EcoRI* polymorphic RFLP identified in the *pre2-2* allele as compared to its WT sib was cloned by making λ library and sequenced using GSPs from the exon8 and exon9 and T7 forward and reverse primers. Total RNA of the *pre2-2* allele along with its WT sibs in BC3F3 was extracted using 10 days old seedlings by growing in paper towels and used for RT-PCR analysis.

4.3 | RNA isolation and RT-PCR

Total RNA was isolated from leaf tissues using the RNeasy plant mini kit (Qiagen). First-strand cDNA was synthesized using QuantiTec reverse transcription kit (Qiagen). The RNA samples



were confirmed to be gDNA free when only cDNA corresponding amplicons but no gDNA amplicons were detected after PCR, using *ZmActin1* primers that can amplify both cDNA and gDNA templates simultaneously, yielding amplicons of different sizes. To amplify the *ZmActin1* fragment in RT-PCR, the *ZmActin1-F* (5'-CTGACGAGGATATCCAGCCTATCGTATGTGACAATG-3') and *ZmActin1-R* (5'-AACCGTGTGGCTCACACCATCACC-3') primers were used. To normalize the first-strand cDNA, the *ZmActin-F1* and *ZmActin1-R* were used in RT-PCR and then GSPs from maize to amplify transcripts of *pre2-1* and *pre2-2* and their WT sibs. Two microliters of the reverse transcription reaction products were used for RT-PCR with gene-specific primers. RT-PCR program consisted of 95°C for 2 min, 35 cycles of 95°C for 15 s, 64°C for 15 s, 72°C for 30 s, and final extension at 72°C for 7 min in a 25- μ l volume. Similarly, amplification of Arabidopsis actin was used as a control in PCR-fingerprinting and the GSPs and actin primers sequence are provided in Table S2.

4.4 | Sequence analysis

Sequence alignments and percent identity calculations were performed using the MEGALIGN® program of the LASERGENE® bioinformatics computing suite (DNASTAR® Inc., Madison, Wis.) and BioEdit (alignment output program). Multiple alignment of the sequences was performed using the ClustalW method of alignment (Higgins & Sharp, 1989) with the default parameters (GAP PENALTY = 10, GAP LENGTH PENALTY = 10). Default parameters for pairwise 60 alignments using the ClustalW method were KTUPLE = 1, GAP PENALTY = 3, WINDOW = 5, and DIAGONALS SAVED = 5. Some proteins were extracted from Phytozyme.

4.5 | Statistical analysis

The phenotypic and agronomic traits data were statistically analyzed for mean, SDs, and SEs. The histograms were prepared using averages and SEs to depict differences between the mutant and their WT sibs. The mean differences between the mutant and wild-type sibs were also compared using unpaired *t* test at both 0.05% and 0.01% level of significances. Segregation ratios were tested using χ^2 analysis. Z scores were calculated to compare the mean differences of transgene plants versus their wild-type null controls. The 2-sigma score was used for the performance of the mutant and/or Ox transgene in comparison to its null WT sib controls. The 2-sigma score greater than 0.9 with a positive standard deviation is considered an outlier in the drought assay in all flats, indicating that the mutant plants outperformed significantly better than their WT sibs used as control.

4.6 | Vector construction and transgene studies

The coding sequence of the *ZmPre2* was used to generate overexpression and RNAi vectors using Gateway cloning. MOPAT driven by ZM-UBI promoter and PMI driven by OsACTIN promoter were

used as selectable markers. A full-length mRNA amplified by RT-PCR (Figure 2b) was used to make overexpression cassette whereas only 450 bp (from 1,189 to 1,638 nucleotides of the *ZmPre2*-cDNA) was used in sense and antisense orientation with an intron (ST-SL2 intron2) as a spacer to make an inverted repeat/RNAi cassette. Both overexpression (Ox) and RNAi constructs were driven using the ZM-UBI promoter. In addition, RFP (red fluorescent protein) driven by a pericarp-specific promoter LTP2 was also used to sort out the transgenic fluorescent red seeds from their segregating non-transgenic sib seeds. The plasmid was then co-integrated into the binary vector in *Agrobacterium tumefaciens* strain LBA4404 (Komari et al., 1996) by electroporation. Transgenic events were generated produced in Hill x Gaspe by *Agrobacterium*-mediated transformation as described (Zhao et al., 2001). Ten transgenic events were characterized at the molecular level for transgene copy number and gene expression by qPCR and single copy transgene events were tested in drought stress and NUE reproductive assays. For phenotypic data on leaf area, leaf color, height, etc., digital images of the plants at various growth stages were recorded. Data on the total biomass and stay green traits were calculated by measuring the leaf area in terms of the number of green pixels obtained using a commercially available imaging system. The percent change in transgene versus null for days to shed, days to silk, and silk count traits were measured. Data for other traits such as ear length, ear width, maximum ear area, and total seed number were obtained at the time of harvesting using Ear Photometry (Hausmann et al., 2007). The relative chlorophyll content was measured by CCM-200 in CCI units (Chlorophyll Content Index). It is a relative measurement of chlorophyll content based on optical absorbance in two different wavelengths: 653 nm and 931 nm. Phenotypic data were analyzed by applying paired *t* test and presented as Z-score.

4.7 | Molecular characterization of Arabidopsis T-DNA insertional knockout allele

Seed of the SALK_017615, SALK_079273, and SALK_107247 mutant lines was obtained from the Arabidopsis Biological Resource Center (ABRC) and subjected to PCR fingerprinting. The GSPs in combination with T-DNA primer were used to confirm the T-DNA insertion sites in the At1G72390 gene. The homozygous knockout mutants and its WT sib plants in SALK_017615 were identified using two GSPs, P1233 and P1234 from exon10 and exon11 of the At1G72390 sequence, respectively, and GSPs in combination with a T-DNA-specific primer (P1052). The sequences of these primers are provided in Table S2.

4.8 | Overexpression of the *ZmPre2* in Arabidopsis

Multisite Gateway (Invitrogen, USA) technology was used to generate plant expression vectors. The coding sequence of *ZmPre2* was amplified by PCR using forward and reverse GSPs (GSP-F + GSP-R) and cloned in pENTR/D-TOPO (Thermo Fisher Scientific, USA). The final expression vector contained herbicide and fluorescent marker for



transgenic seed sorting. Quality check was performed on the resulting expression vector by restriction digestion mapping and transferred into *Agrobacterium tumefaciens* LB4404JT by electroporation. The co-integrated DNA from transformed *Agrobacterium* was transferred in *E. coli* DH10B and the plasmid DNA from this strain was used to check its quality again by restriction digestion. These overexpression vectors were transformed into *Arabidopsis thaliana* ecotype Columbia-0 by *Agrobacterium*-mediated "Floral-Dip" method (Clough & Bent, 1998). T0 seeds were screened for T1 transformants in soil for herbicide resistance. For molecular analysis of the transgenic T1 events, RT-PCRs were conducted to detect the transgene expression, actin control, and the presence of genomic DNA in the RNA preparations. Transgene expressing plants were advanced and screened in drought assay.

4.9 | Characterization of *Arabidopsis* transgenic and knockout alleles under drought stress

Drought assay was performed on a total of 72 mutants and 72 wild-type sibs (WT) by eight pots (cells) for each. Each pot was sown to produce nine mutants or nine WT seedlings in a 3 × 3 array. Flats are configured with eight square pots each in one experiment. Each pot was filled with Metro-Mix® 200 soil (Sun Gro, USA). The seed was imbibed in liquid and placed at 4°C for 48+ hours to ensure uniform germination before placing it into the growth chamber. The soil was watered to saturation and then plants were grown under standard conditions of 16h light, 8h dark cycle; 22°C; 60% relative humidity). No additional water was given after day 16. Digital images of the plants were taken at the onset of visible drought stress symptoms. Images were taken once a day (at the same time every day), until the plants appear desiccated. Typically, four consecutive days of data are captured. Color analysis was employed for identifying potential drought-tolerant lines. Maintenance of leaf area over time, as described in Shi et al. (2015), was used as a criterion for identifying potential drought-tolerant lines. Leaf area was measured in terms of the number of green pixels obtained using an imaging system. Mutant and control (wild type) plants were grown side by side in flats and when wilting begins. From these data, wilting profiles were determined based on the green pixel counts obtained over four consecutive days for transgene or knockout mutant plants and accompanying control plants. The profile was selected from a series of measurements over the day-4 period that provided the largest degree of wilting. The ability to withstand drought was measured by the tendency of plants to resist wilting compared to their control WT sib plants.

4.10 | Characterization of *Arabidopsis* knockout allele on low and high nitrogen

For Low N plate assays, 32 mutant and 32 wild-type plants were grown on square plates (15 mm × 15 mm) containing 0.5x N-Free Hoagland's, 0.4 mM potassium nitrate, 0.1% sucrose, 1 mM MES and 0.25% Phytigel™ (Low N medium). Plates were kept for 3 days in the

dark at 4°C to stratify seeds and then placed horizontally for 9 days at 22°C light and 20°C dark. Plates were placed under 16 hr light and 8 hr dark, with an average light intensity of ~200 mmol/m²/s. Plates were rotated and shuffled daily within each shelf. On day 12 (9 days of growth), seedling status was evaluated by imaging the entire plate. After masking the plate image to remove background color, two different measurements were collected for each individual plant: total rosette area, and the percentage of color that falls into a green color bin using hue, saturation, and intensity data (HSI). The green color bin consists of hues 50–66. Total rosette area was used as a measure of plant biomass, whereas the green color bin was shown by dose-response studies to be an indicator of nitrogen assimilation.

4.11 | Characterization of *Arabidopsis* knockout allele for ABA response

Seeds of knockout mutant and Col-0 WT (36 seeds of each mutant and WT with three replications) were grown on half MS media (without sucrose) with or without abscisic acid (1 μM ±-cis, trans-ABA). The plates with seeds were kept at 4°C in dark for 3 days and then incubated in the growth chamber under the long-day growth conditions (16h-light/8h-dark cycle at 120–150 μmol/m² s⁻¹ and 20°C to 22°C, with 75% humidity). Visible radicle tips (1–2 mm) were counted after 48h as a germinated seed. Data on seed germination were analyzed by calculating means and SEs and applying *t* test.

ACKNOWLEDGMENTS

We are thankful for the greenhouse regular and contractual workers at Johnston, IA and Experimental Station, Wilmington, DE, who have helped us in recording data on various traits and capturing digital images in different maize and *Arabidopsis* experiments. We would also like to thank both Mark Mucha and Ryan J. Yule for evaluating the *AtPre2-KO* mutant and its WT-sib seed using horizontal Low N media for NUE and vertical High N media plates for root inhibition assays, respectively.

CONFLICTS OF INTEREST

I would also like to disclose that I might have conflict as a potential reviewer with Dr. G. S. Johal, Department of Botany and Plant Pathology, Purdue University, West Lafayette, Indiana due to our past collaboration, publishing a research paper together on agronomic traits such as dwarfing genes in *Science* (Multani, Briggs et al., 2003), and as co-authors on *brittle stalk2* in *Plant Physiology* (Sindhu et al., 2007). Similarly, there would be a potential conflict of interest with my former collaborators at Corteva Agriscience; Drs. Jeffery E. Habben, Renee H. Lafitte, Michael G. Muszynski, and Kanwarpal S Dhugga. Rajeev Gupta has a specific conflict with his class fellow, Dr. R. S. Sekhon, Department of Genetics and Biochemistry, Clemson University, Clemson, SC 29634, USA, due to close friendship. The findings reported in this study were filed in a patent which has been published under the title, "Plants with improved agronomic traits" in the United States Patent No. 9,422,572 B2 issued on Aug. 23, 2016 (Allen et al., 2016).



AUTHOR CONTRIBUTIONS

R.G. Acquired seed of Arabidopsis T-DNA insertion mutants, their characterization, and assisted in manuscript preparation; S.J. Candidate gene validation, RT-PCR, preparation of graphs, figures, and tables; S.Z. Candidate gene isolation, RT-PCR of the *pre2* mutants, and isolated FL-cDNA of *Pre2*. R.B.M. Isolated *pre2-1* mutant, provided resources, and guidance for this research project; R.W.W. Overexpression of the maize *Pre2* candidate gene in Arabidopsis, and testing Arabidopsis knockout mutants and transgenes for drought stress; D.F. helped Shuping in various experiments in the greenhouse; G.T. Evaluated Arabidopsis knockout mutant for NUE; G.L. Characterization of overexpressing and RNAi transgenes of *ZmPre2* in FASTCORN; J.L. Evaluated Arabidopsis knockout mutant in ABA assay; S.M.A. Assisted R.W.W. in drought testing, identified homolog sequences in other plant species; K.D.S. Obtained germplasm, managed field nurseries, and assisted in manuscript preparation; D.S.M. Candidate gene isolation and validation, supervised both SJ and SZ, data analysis, filed IP, and prepared this manuscript.

FUNDING INFORMATION

This work was supported by Corteva Agriscience.

ORCID

Rajeev Gupta  <https://orcid.org/0000-0002-1451-215X>
 Shuping Jiao  <https://orcid.org/0000-0001-8917-9876>
 Suling Zhao  <https://orcid.org/0000-0003-1799-8033>
 Robert B. Meeley  <https://orcid.org/0000-0002-4496-1888>
 Robert W. Williams  <https://orcid.org/0000-0002-6044-4952>
 Graziana Taramino  <https://orcid.org/0000-0001-6544-097X>
 Dongsheng Feng  <https://orcid.org/0000-0002-9871-2107>
 Guofu Li  <https://orcid.org/0000-0002-7631-6285>
 Juan Liu  <https://orcid.org/0000-0003-4804-8276>
 Stephen M. Allen  <https://orcid.org/0000-0002-5232-1987>
 Kevin D. Simcox  <https://orcid.org/0000-0002-0683-7034>
 Dilbag S. Multani  <https://orcid.org/0000-0003-2343-4613>

REFERENCES

- Allen, S. M., Gupta, R., Jiao, S., Meeley, R. B., Multani, D. S., & Williams, R. (2016). Plants with improved agronomic traits. US Patent Number US9422572B2, Issued on Aug. 23, 2016.
- Bot, A. J., Nachtergaele, F. O., & Young, A. (2000). Land resource potential and constraints at regional and country levels. *World Soil Resources Reports*, 90, 114.
- Breeze, E., Harrison, E., McHattie, S., Hughes, L., Hickman, R., Hill, C., Kiddle, S., Kim, Y.-S., Penfold, C. A., Jenkins, D., Zhang, C., Morris, K., Jenner, C., Jackson, S., Thomas, B., Tabrett, A., Legaie, R., Moore, J. D., & Wild, D. L., & Buchanan-Wollaston, V. (2011). High-resolution temporal profiling of transcripts during Arabidopsis leaf senescence reveals a distinct chronology of processes and regulation. *The Plant Cell*, 23, 873–894. <https://doi.org/10.1105/tpc.111.083345>
- Brugière, N., Zhang, W., Xu, Q., Scolaro, E. J., Lu, C., Kahsay, R. Y., Kise, R., Trecker, L., Williams, R. W., Hakimi, S., Niu, X., Lafitte, R., & Habben, J. E. (2017). Overexpression of Ring domain E3 ligase *ZmXeric1* confers drought tolerance through regulation of ABA homeostasis. *Plant Physiology*, 175, 1350–1369. <https://doi.org/10.1104/pp.17.01072>
- Buchanan-Wollaston, V., Earl, S., Harrison, E., Mathas, E., Navabpour, S., Page, T., & Pink, D. (2003). The molecular analysis of leaf senescence—A genomics approach. *Plant Biotechnology Journal*, 1, 3–22. <https://doi.org/10.1046/j.1467-7652.2003.00004.x>
- Buchanan-Wollaston, V., Page, T., Harrison, E., Breeze, E., Lim, P. O., Nam, H. G., Lin, J. F., Wu, S. H., Swidzinski, J., Ishizaki, K., & Leaver, C. J. (2005). Comparative transcriptome analysis reveals significant differences in gene expression and signaling pathways between developmental and dark/starvation-induced senescence in Arabidopsis. *The Plant Journal*, 42, 567–585. <https://doi.org/10.1111/j.1365-313x.2005.02399.x>
- Chai, M., Guo, Z., Shi, X., Li, Y., Tang, J., & Zhang, Z. (2019). Dissecting the regulatory network of leaf premature senescence in maize (*Zea mays* L.) using transcriptome analysis of *ZmEL55* mutant. *Genes*, 10, 944. <https://doi.org/10.3390/genes10110944>
- Clough, S. J., & Bent, A. F. (1998). Floral dip: A simplified method for Agrobacterium-mediated transformation of *Arabidopsis thaliana*. *The Plant Journal*, 16, 735–743. <https://doi.org/10.1046/j.1365-313x.1998.00343.x>
- Deikman, J., Petracek, M., & Heard, J. E. (2012). Drought tolerance through biotechnology: Improving translation from the laboratory to farmers' fields. *Current Opinions in Biotechnology*, 23, 243–250. <https://doi.org/10.1016/j.copbio.2011.11.003>
- Dooner, H. K., Wang, Q., Huang, J. T., Li, Y., He, L., Xiong, W., & Du, C. (2019). Spontaneous mutations in maize pollen are frequent in some lines and arise mainly from retro transpositions and deletions. *Proceedings of the National Academy of Sciences of the United States of America*, 116, 10734–10743. <https://doi.org/10.1073/pnas.1903809116>
- Endo, M., Kudo, D., Koto, T., Shimizu, H., & Araki, T. (2014). Light-dependent destabilization of PHL in Arabidopsis. *Plant Signaling & Behavior*, 9, e28118. <https://doi.org/10.4161/psb.28118>
- Endo, M., Tanigawa, Y., Murakami, T., Arakia, T., & Nagatani, A. (2013). PHYTOCHROME-DEPENDENT LATE-FLOWERING accelerates flowering through physical interactions with phytochrome B and CONSTANS. *Proceedings of the National Academy of Sciences of the United States of America*, 110, 18017–18022. <https://doi.org/10.1073/pnas.1310631110>
- Fassler, J. S., & Winston, F. (1989). The *Saccharomyces cerevisiae* SPT13/GAL11 gene has both positive and negative regulatory roles in transcription. *Molecular and Cellular Biology*, 9(12), 5602–5609.
- Gollmack, D., Li, C., Mohan, H., & Probst, N. (2014). Tolerance to drought and salt in plants: Unraveling the signaling networks. *Frontiers of Plant Science*, 5, 151. <https://doi.org/10.3389/fpls.2014.00151>
- Guo, Y., Cai, Z., & Gan, S. (2004). Transcriptome of Arabidopsis leaf senescence. *Plant, Cell and Environment*, 27, 521–549. <https://doi.org/10.1111/j.1365-3040.2003.01158.x>
- Han, M., Okamoto, M., Beatty, P. H., Rothstein, S. J., & Good, A. G. (2015). The genetics of nitrogen use efficiency in crop plants. *Annual Review of Genetics*, 49, 269–289. <https://doi.org/10.1146/annurev-genet-112414-055037>
- Hausmann, N. J., Abadie, T. E., Cooper, M., Lafitte, H. R., & Schuller, J. R. (2007). Method and system for digital image analysis of ear traits. Publication No. 20090046890; Patent Grant No. 8073235.
- Higgins, D. G., & Sharp, P. M. (1989). Fast and sensitive multiple sequence alignments on a microcomputer. *Computer Applications in the Biosciences*, 5, 151–153. <https://doi.org/10.1093/bioinformatics/5.2.151>
- Himelblau, E., & Amasino, R. M. (2001). Nutrients mobilized from leaves of Arabidopsis thaliana during leaf senescence. *Journal of Plant Physiology*, 158, 1317–1323. <https://doi.org/10.1078/0176-1617-00608>
- Hoopes, G. M., Hamilton, J. P., Wood, J. C., Esteban, E., Pasha, A., Vaillancourt, B., Provart, N. J., & Buell, C. R. (2019). An updated gene atlas for maize reveals organ-specific and stress-induced genes. *The Plant Journal*, 97, 1154–1167. <https://doi.org/10.1111/tj.14184>
- Jiao, S., Hazebroek, J. P., Chamberlin, M. A., Perkins, M., Sandhu, A. S., Gupta, R., Simcox, K. D., Yinghong, L. I., Prall, A., Heetland, L., Meeley, R. B., & Multani, D. S. (2019). *Chitinase-like1* plays a role in stalk tensile strength in maize. *Plant Physiology*, 181, 1127–1147. <https://doi.org/10.1104/pp.19.00615>



- Komari, T., Hiei, Y., Saito, Y., Murai, N., & Kumashiro, T. (1996). Vectors carrying two separate T-DNAs for co-transformation of higher plants mediated by *Agrobacterium tumefaciens* and segregation of transformants free from selection markers. *The Plant Journal*, *10*, 165–174. <https://doi.org/10.1046/j.1365-313x.1996.10010165.x>
- Koutelou, E., Hirsch, C. L., & Dent, S. Y. (2010). Multiple faces of the SAGA complex. *Current Opinions in Cell Biology*, *22*, 374–382. <https://doi.org/10.1016/j.ceb.2010.03.005>
- Kumar, V., Waseem, M., Dwivedi, N., Maji, S., Kumar, A., & Thakur, J. K. (2018). KIX domain of AtMed15a, a mediator subunit of Arabidopsis, is required for its interactions with different proteins. *Plant Signaling & Behavior*, *13*(2), e1428514. <https://doi.org/10.1080/15592324.2018.1428514>
- Lee, I. C., Hong, S. W., Whang, S. S., Lim, P. O., Nam, H. G., & Koo, J. C. (2011). Age-dependent action of an ABA-inducible receptor kinase, RPK1, as a positive regulator of senescence in Arabidopsis leaves. *Plant Cell Physiology*, *52*, 651–662. <https://doi.org/10.1093/pcp/pcr026>
- Lee, T. I., Causton, H. C., Holstege, F. C. P., Shen, W.-C., Hannett, N., Jennings, E. G., Winston, F., Green, M. R., & Young, R. A. (2000). Redundant roles for the TFIID and SAGA complexes in global transcription. *Nature*, *405*, 701–707. <https://doi.org/10.1038/35015104>
- Li, H., Hu, B., & Chu, C. (2017). Nitrogen use efficiency in crops: Lessons from Arabidopsis and rice. *Journal of Experimental Botany*, *68*, 2477–2488. <https://doi.org/10.1093/jxb/erx101>
- Lim, P. O., Kim, H. J., & Nam, H. G. (2007). Leaf senescence. *Annual Review of Plant Biology*, *58*, 115–136. <https://doi.org/10.1146/annurev.arplant.57.032905.105316>
- Liu, X., Li, Z., Jiang, Z., Zhao, Y., Peng, J., Jin, J., Guo, H., & Luo, J. (2011). LSD: A leaf senescence database. *Nucleic Acids Research*, *39*, D1103–D1107. <https://doi.org/10.1093/nar/gkq1169>
- Moraga, F., & Aquea, F. (2015). Composition of the SAGA complex in plants and its role in controlling gene expression in response to abiotic stresses. *Frontiers of Plant Science*, *6*, 865. <https://doi.org/10.3389/fpls.2015.00865>
- Multani, D. S., Briggs, S. P., Chamberlin, M. A., Blakeslee, J. J., Murphy, A. S., & Johal, G. S. (2003). Loss of an MDR Transporter in Compact Stalks of Maize br2 and Sorghum dw3 Mutants. *Science*, *302*(5642), 81–84. <http://dx.doi.org/10.1126/science.1086072>
- Multani, D. S., Lee, Y., & Johal, G. S. (2003). The premature senescence mutant (*pre1*) maps to the long arm of chromosome 1. *Maize Genetics Cooperative Newsletter*, *77*, 45. <https://mnl.maizegdb.org/mnl/77/02multani.html>
- Muszynski, M. G., Dam, T., Li, B., Shirbroun, D. M., Hou, Z., Bruggemann, E., & Danilevskaia, O. N. (2006). *Delayed flowering1* encodes a basic leucine zipper protein that mediates floral inductive signals at the shoot apex in maize. *Plant Physiology*, *142*, 1523–1536. <https://doi.org/10.1104/pp.106.088815>
- Nagy, Z., Riss, A., Romier, C., le Guezennec, X., Dongre, A. R., Orpinell, M., Han, J., Stunnenberg, H., & Tora, L. (2009). The human SPT20-containing SAGA complex plays a direct role in the regulation of endoplasmic reticulum stress-induced genes. *Molecular and Cellular Biology*, *29*, 1649–1660. <https://doi.org/10.1128/MCB.01076-08>
- Omara, P., Aula, L., Oyebiyi, F., & Raun, W. R. (2019). World cereal nitrogen use efficiency trends: Review and current knowledge. *Agrosystems, Geosciences & Environment*, *2*, 1–8. <https://doi.org/10.2134/age2018.10.0045>
- Piskacek, S., Gregor, M., Nemethova, M., Grabner, M., Kovarik, P., & Piskacek, M. (2007). Nine-amino-acid transactivation domain: Establishment and prediction utilities. *Genomics*, *89*, 756–768. <https://doi.org/10.1016/j.ygeno.2007.02.003>
- Sade, N., Wilhelmi, M. M., Umnajkitikorn, K., & Blumwald, E. (2018). Stress-induced senescence and plant tolerance to abiotic stress. *Journal of Experimental Botany*, *69*, 845–853. <https://doi.org/10.1093/jxb/erx235>
- Schaefer, M., Wanker, E. E., & Andrade-Navarro, M. A. (2012). Evolution and function of CAG/polyglutamine repeats in protein-protein interaction networks. *Nucleic Acids Research*, *40*, 4273–4287. <https://doi.org/10.1093/nar/gks011>
- Sekhon, R. S., Sasaki, C., Kumar, R., Flinn, B. S., Luo, F., Beissinger, T. M., Ackerman, A. J., Breitzman, M. W., Bridges, W. C., de Leon, N., & Kaeppler, S. M. (2019). Integrated genome-scale analysis identifies novel genes and networks underlying senescence in maize. *The Plant Cell*, *31*, 1968–1989. <https://doi.org/10.1105/tpc.18.00930>
- Sen, A., Hsieh, W.-C., & Aguilar, R. C. (2017). The Information content of glutamine-rich sequences define protein functional characteristics. *Proceedings of the IEEE*, *105*, 385–393. <https://doi.org/10.1109/JPROC.2016.2613076>
- Shi, J., Habben, J. E., Archibald, R. L., Drummond, B. J., Chamberlin, M. A., Williams, R. W., Lafitte, H. R., & Weers, B. P. (2015). Overexpression of ARGOS Genes modifies plant sensitivity to ethylene, leading to improved drought tolerance in both Arabidopsis and maize. *Plant Physiology*, *169*, 266–282. <https://doi.org/10.1104/pp.15.00780>
- Srivastava, R., Rai, K. M., Pandey, B., Singh, S. P., & Sawant, S. V. (2015). Spt-Ada-Gcn5-Acetyltransferase (SAGA) complex in plant genome wide identification, evolutionary conservation, and functional determination. *PLoS One*, *10*, e01334709. <https://doi.org/10.1371/journal.pone.0134709>
- Suzuki, Y., Nogi, Y., Abe, A., & Fukasawa, T. (1988). GAL11 protein, an auxiliary transcription activator for genes encoding galactose-metabolizing enzymes in *Saccharomyces cerevisiae*. *Molecular and Cellular Biology*, *8*(11), 4991–4999. <https://doi.org/10.1128/MCB.8.11.4991>
- Takahashi, H., Sun, X., Hamamoto, M., Yashiroda, Y., & Yoshida, M. (2012). The SAGA histone acetyltransferase complex regulates leucine uptake through the App3 permease in fission yeast. *Journal of Biological Chemistry*, *287*, 38158–38167. <https://doi.org/10.1074/jbc.M112.411165>
- van der Graaff, E., Schwacke, R., Schneider, A., Desimone, M., Flügge, U.-I., & Kunze, R. (2006). Transcription analysis of Arabidopsis membrane transporters and hormone pathways during developmental and induced leaf senescence. *Plant Physiology*, *141*, 776–792. <https://doi.org/10.1104/pp.106.079293>
- Woo, H. R., Kim, H. J., Lim, P. O., & Nam, H. G. (2019). Leaf senescence: Systems and dynamics aspects. *Annual Review of Plant Biology*, *70*, 347–376. <https://doi.org/10.1146/annurev-arplant-050718-095859>
- Zhang, J., Fengler, K. A., Van Hemert, J. L., Gupta, R., Mongar, N., Sun, J., Allen, W. B., Wang, Y., Weers, B., Mo, H., Lafitte, R., Hou, Z., Bryant, A., Ibraheem, F., Arp, J., Swaminathan, K., Moose, S. P., Li, B., & Shen, B. (2019). Identification and characterization of a novel stay-green QTL that increases yield in maize. *Plant Biotechnology Journal*, *17*, 2272–2285. <https://doi.org/10.1111/pbi.13139>
- Zhao, Z., Gu, W., Cai, T., Tagliani, L., Hondred, D., Bond, D., Schroeder, S., Rudert, M., & Pierce, D. (2001). High throughput genetic transformation mediated by *Agrobacterium tumefaciens* in maize. *Molecular Breeding*, *8*, 323–333. <https://doi.org/10.1023/A:1015243600325>

SUPPORTING INFORMATION

Additional supporting information may be found online in the Supporting Information section.

How to cite this article: Gupta R, Jiao S, Zhao S, et al. The maize *premature senescence2* encodes for *PHYTOCHROME-DEPENDENT LATE-FLOWERING* and its expression modulation improves agronomic traits under abiotic stresses. *Plant Direct*. 2020;00:1–18. <https://doi.org/10.1002/pld3.295>